Elastic Stress Effects on Microstructural Instabilities

M.P. Gururajan[1]* and Arka Lahiri[2]

Abstract | Phase field modelling, which is ideal for the study of the formation and evolution of microstructures, has been used extensively to study the effect of elastic stresses on microstructural instabilities. In this review, we focus primarily on four elastic stress driven instabilities, namely (i) Spinodal phase separation; (ii) Particle splitting; (iii) Rafting; and, (iv) Asaro-Tiller-Grinfeld (ATG) instabilities, and, review the phase field studies of these instabilities. The review begins with a brief description of some of the important and interesting experimental observations followed by a reasonably detailed description of the theoretical developments. Both the description of experimental observations and the theoretical developments are neither comprehensive nor complete; however, they are helpful in setting the stage for discussion of (and, in giving a perspective on) phase field modelling studies on elastic stress effects on instabilities. We conclude with a summary and indication of future directions.

1 Introduction

Microstructure (which, for the purposes of this article, defined as the sizes, shapes and distributions of interfaces in a material) is the key bridge between processing and properties. Hence, a study of the formation and evolution of microstructures is of great interest: see, for example,[1] and references therein. Naturally, during the formation and evolution of microstructures, new interfaces may form and old ones might disappear; in addition, interfaces might merge or split.

Instabilities is one of the key phenomenon that leads to interesting microstructural features; for example, compositional instabilities in binary alloys aged inside the spinodal region of a miscibility gap leading to spinodal microstructures and dendritic microstructures result from the breaking up of planar solid-liquid interfaces during solidification. Martin, Doherty and Cantor, in their monograph on microstructural stability[2]

give a fairly comprehensive list of microstructural instabilities and classify them as due to chemical energy, strain energy, interfacial energy and others (such as irradiation, magnetic, thermal and electric fields). Our interest in this review is on microstructural instabilities that are influenced by elastic stresses.

Elastic stress effects on microstructures are well known—see, for example the articles[3–6] or the monographs of Mura[7] and Khachaturyan.[8] Elastic stresses arise naturally during phase transformations (for example, lattice parameter mismatch in coherent precipitates), processing (for example, during the epitaxial growth of a thin film on a rigid substrate) and/or service and environmental conditions (for example, stressed minerals that are in contact with their solutions). Elastic stresses play two distinct roles in influencing microstructural instabilities—namely, promotion and suppression of instabilities; the Asaro-Tiller-

[1]*Department of Metallurgical Engineering and Materials Science, Indian Institute of Technology Bombay, Powai, Mumbai, 400076, India.*

[2]*Department of Materials Engineering, Indian Institute of Science, Bengaluru, 560012, India.*

*gururajan.mp@gmail.com, guru.mp@iitb.ac.in

REVIEWS

Grinfeld (ATG) instabilities is a typical example of stress induced instability while the suppression of spinodal decomposition is a typical example of stress induced suppression.

Phase field models are ideal for the study of formation and evolution of microstructures. In these models, also known as diffuse interface models, the interfaces are not explicitly tracked. So, any topological singularity associated with the formation, merger, splitting and disappearance of interfaces can be handled smoothly. Further, interfaces are defects and hence have a positive excess free energy associated with them. In phase field models, this excess free energy associated with them can be incorporated and thus any interface related physics (such as Gibbs-Thomson effect, for example) can be automatically accounted for. Hence, phase field models have been extensively used in the past two decades for studying a variety of systems and their microstructures—see[9-17] for some reviews.

This review is on the phase field modelling studies in elastic stress effects on microstructural instabilities. We will focus primarily on four elastic stress driven instabilities:

1. Spinodal phase separation;
2. Particle splitting;
3. Rafting; and,
4. Asaro-Tiller-Grinfeld (ATG) instabilities

In systems that undergo elastic stress driven microstructural instabilities, the different constituent phase might have different moduli (that is, the system is elastically inhomogeneous); (coherency driven) eigenstrains might be present; and, there might be applied traction (or imposed strains) on the system. Even though all these three might be present in all these four problems, for the instability to occur, one (or more) of these is (are) essential. For example, elastic inhomogeneity along with imposed strains/applied stresses is sufficient to produce ATG instabilities; rafting requires all three—namely, eigenstrain, elastic inhomogeneity and applied stresses, and in the absence of any of these it will not occur; and, suppression of spinodal and particle splitting can take place in the presence of eigenstrains (even if there are no applied stresses, or imposed strains and/or elastic moduli mismatch).

Spinodal phase separation: spontaneous phase separation of a homogeneous phase into a mechanical mixture of two phases.

There are several other microstructural instabilities, such as dendritic formation during solid-solid phase transformations,[18-20] buckling and wrinkling of soft films[21] and liquid crystal elastomers,[22] twinning,[23-25] dissolution-precipitation creep at grain boundaries in minerals,[26] phase inversion,[27-28] dynamic brittle fracture[29] and branching instability, cracking of surfaces,[30] dissolution driven crack growth,[31] surface roughening instability during dynamic fracture,[32] step instabilities (bunching and undulation) on stressed surface,[33] stress driven roughening of solid-solid interfaces,[34] the destabilization of solidification and melting fronts due to stress,[35] dynamical instabilities of dislocation patterning in fatigued metals,[36] crystals growing on curved surfaces,[37] stress induced boundary motion,[38] martensitic transformations,[39] microstructural evolution in systems with cracks and voids[40-43] and so on. In many of these instabilities elastic stresses might play an important role. However, in this review, we do not discuss them.

This review is organised as follows: in Section 2, we briefly describe some of the important and interesting experimental observations on elastic stress effects on microstructural instabilities; in Section 3, we describe, in reasonable detail, the theoretical developments in understanding the effects of elastic stress on microstructural instabilities in solids. Section 2 and 3 are neither comprehensive nor complete; however, they are helpful in setting the stage for discussion of (and, in giving a perspective on) phase field modelling studies that will be discussed in Section 4. In Section 5, we conclude with a summary and indication of future directions.

2 Experimental Observations

The elastic stress driven microstructural instabilities are of great practical importance; the stress-corrosion cracking of minerals in earth's mantle, instabilities during the growth of thin films, formation of quantum dots, particle splitting and rafting in Ni-base superalloys, and suppression of spinodal decomposition are but some of the well-known stress driven microstructural instabilities of relevance. In this section, as noted earlier, we very briefly indicate some of the important experimental observations—in order to set the stage for a detailed discussion of the theoretical and phase field studies. The description here is neither complete nor comprehensive; the interested reader is referred to references[2-6] for more information.

2.1 *Spinodal phase separation: Suppression and promotion*

It is fairly well known that elastic stresses can suppress microstructural instabilities; for example, such suppression is reported in Al-Zn,[44-45] Au-Pt

alloys[46] alkali feldspars (specifically, sanidine-high albite systems),[47] semiconductors doped with transition metals,[48] Ci-Ni(Fe) nanolaminates[49] and pyroxenes.[50]

On the other hand, self-assembled quantum dots and wires in epitaxially grown thin films are produced using spinodal decomposition mechanism; see[51] (and, some of the references therein).[52–61] However, in some of these systems, the effect of epitaxial strain on spinodal instability is asymmetric—for example, compressive stresses might promote phase separation[54,61] while tensile stresses suppress the same.[62,63]

2.2 Particle splitting

Elastic stress induced splitting instability of misfitting precipitates have been reported[64–71] in several Ni-base systems. The particle splitting instability is the opposite of coarsening; as the size becomes larger than some critical value, the precipitate splits into doublets, quartets or octets; see,[72] for an example of the wide variety of split structures that are observed.

There are also a few studies that question the interpretation of particle splitting; instead it is explained as a coalescence induced[73–75] or compositional heterogeneity induced (albeit in Ir-Nb system)[76] microstructural feature. As we discuss later, there is phase field modelling based evidence supporting both the splitting and coalescence mechanisms.

2.3 *Rafting*

In Ni-base superalloys consisting of γ' precipitates (with L1$_2$, an ordered face centered cubic crystal structure) in nickel rich γ (disordered fcc) matrix (as well as others with a similar microstructure of coherent ordered precipitates in a disordered matrix), under an applied uniaxial stress, rafting (which is a preferential coarsening) is one of the instabilities seen: see, for example[77–83] and the reviews of Chang and Allen[84] and Kamaraj.[85] During rafting, the γ' precipitates coarsen preferentially under the action of the applied load—either parallel or perpendicular to the direction of applied load if it is uniaxial; if the loading is not uniaxial, the rafting is more complex.[80]

Rafting leads to the destruction of an initially periodic arrangement of cuboids of precipitates during service, and leads to a microstructure consisting of wavy precipitates with very large aspect ratios. Depending on the type of microstructure that coarsening leads to, it can lead to either hardening or softening of the microstructure: see for example.[86] In cases of practical importance,

the dislocation mediated plastic flow as well as twinning are known to play a crucial role in this instability: see for example.[87–92] Dislocation activity is also known to help coalesce different variants of ordered precipitates by helping get rid of the anti-phase boundary during rafting.[93] However, phase field models have indicated (as discussed below) that purely elastic stress driven (diffusional) rafting is possible.

2.4 *Asaro-Tiller-Grinfeld (ATG) and associated instabilities*

The surface of any non-hydrostatically stressed solid, in contact with a more compliant phase (be it vapour, liquid or another solid), tends to develop undulations.[94–97] This is broadly known as Asaro-Tiller-Grinfeld (ATG) instability (and will be discussed in some detail in the next section). ATG instabilities are reported in a wide variety of systems and conditions: for example, in Helium IV at the solid-liquid interface,[98] at the surface of SiGe films grown on Si substrates,[99] at the surfaces of polymeric thin films that undergo polymerization,[100] at the interfaces of minerals in contact with their solution,[101–103] on the surface of pure aluminium crystals that undergo cyclic loading[104,105] and in multilayers of systems such as Si-Ge[106,107] and Gadolinia-Silica.[108] The schematic in Fig. 1 (based on)[99] explains the physics behind the ATG instability: if the surface is planar, then, the imposed strains can not relax; however, if the surface develops undulations, then, the imposed strains on the film can relax at the peaks; on the other hand, the stresses at the troughs are more than the flat surface. Hence, the undulations keep growing. In case there is growth in the presence of such undulations, the chemical potentials are such that the atoms would preferentially attach to the peaks.

These instabilities can further be classified as of two types—namely, static and dynamic. In some cases, say, for example the case of minerals in contact with their solution, the ATG instability is static; that is, there is no growth induced movement of the mineral-solution boundary. On the other hand, in the case of SiGe films on Si substrates, the ATG instability is dynamic; that is, ATG is concurrent with the growth of the film and the instability is enhanced by the growth processes.[6] In the case of dynamic instabilities, there could be other elastic field mediated instabilities that are not of the ATG type: for example, Duport, Nozières and Villain[109] report on a step-bunching instability, which is because of elastic

Rafting: preferential coarsening of precipitates under the action of applied traction.
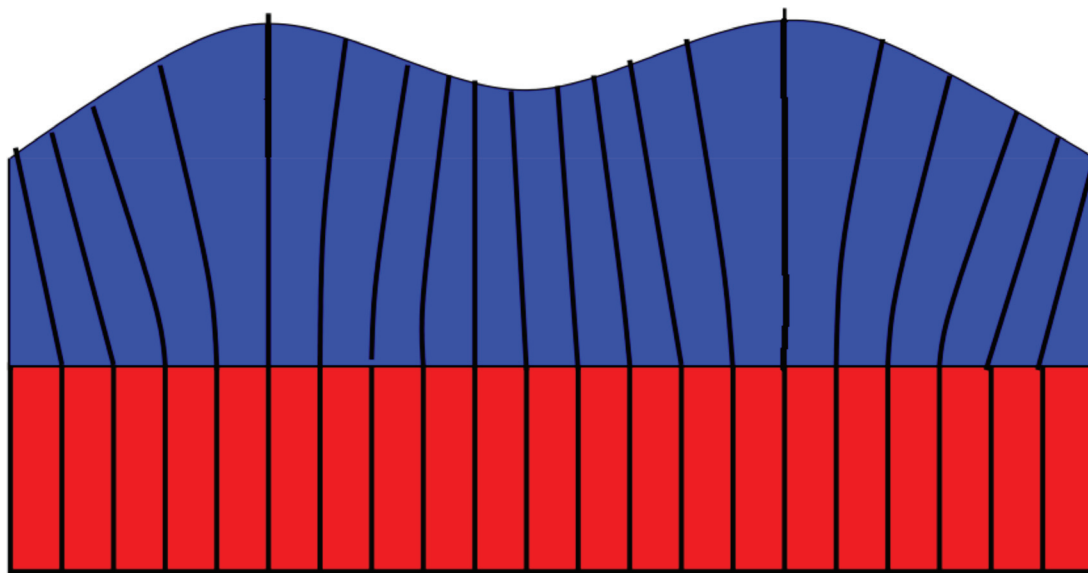
Figure 1: Schematic explaining how the stressed film (due to the lattice parameter of the substrate (red) being imposed on the film (blue)) can relax the stresses at the peaks. However, the stress concentration at the troughs increases. Hence, once the undulation is set-up, it continues to grow.

interaction between adatoms and rest of the material during molecular beam epitaxy (and is different from ATG). In addition, it is known that in confined systems, the dynamics of ATG instabilities could be different.[110]

In the next two sections, we describe the theoretical framework and phase field models that capture several aspects of ATG instabilities. However, the literature on ATG instabilities is too vast to be summarised here. We refer the interested reader to the available monographs[111–113] and reviews[6,114–117] in the literature.

3 Theory and Models

Solids, unlike fluids, can support non-hydrostatic stresses. Hence, the effect of such stresses on the thermodynamics (especially, with specific reference to phase transformations) is of great interest.

As early as 1876, Gibbs[118] alluded to this in his classic work on the equilibrium of heterogeneous substances with one of the sections named as:

The conditions of internal and external equilibrium for solids in contact with fluids with regards to all possible states of strain of the solids.

However, even four decades after Gibbs, that there was no substantial progress on this problem is clear from the following sentences of Bridgman (written in 1916)—quoted from:[119]

The question at issue was: What is the effect on a transition (or melting) point of unknown extra stresses not hydrostatic in nature? It was a surprise to me, after a careful search, to find that this problem has received very meager attention, ...

By 1950s, the contribution of surface stresses to interfacial free energy was recognized.[120] About 45 years after Bridgman's observation, Cahn[121] introduced the idea of coherent spinodal—namely, the suppression of spinodal region due to the elastic stress effects. Larche and Cahn[122] studied the question of equilibrium in stressed solids with specific reference to their interaction with composition in crystalline solids in early 1970s; at around the same time, Asaro and Tiller[94] addressed the question of the equilibrium of a non-hydrostatically stressed solid in contact with its melt.

Around 1984, Johnson and Cahn[123] introduced the idea of elastic stress induced shape bifurcations. Though Asaro and Tiller addressed this question using a perturbation analysis, Grinfeld,[95] independently, in 1986, showed that the question can be posed as an equilibrium problem and answered it using variational analysis; more specifically, Grinfeld showed that the surface of a non-hydrostatically stressed solid (however small the stress be) in contact with its melt will be unstable with respect to fluctuations of any wavelength (in the absence of interfacial energy) and that the lower

wavelength limit of the fluctuations is set by the interfacial energy.

In this section, we discuss the theoretical concepts and formulations in some detail. The rationale behind such a detailed exposition is as follows:

- The complete derivation of elastic stress induced promotion of spinodal is not available in the literature in detail and is being presented here for the first time;
- There are similarities and differences between the approaches; for example, both stress induced suppression of spinodal and ATG instability can be studied using linear stability analyses; ATG instability itself can be studied using both perturbative variational analyses; the Eshelby energy-momentum tensor plays a crucial role in understanding both ATG instabilities and rafting; and so on. Having all the models described in one place helps us gain a perspective which is otherwise missing; and,
- The theoretical concepts and formulations are also important from phase field modelling point of view.
  – The theoretical studies play a foundational role in helping us formulate the phase field models and checking for their correctness;
  – The theoretical studies, since they give analytical solutions under certain simplifying assumptions and approximations, are helpful in benchmarking the implementations of the phase field models; and,
  – The phase field models can be used to systematically relax the constraints imposed or assumptions and approximations made in the theoretical studies; thus, the theoretical studies are helpful in setting the agenda for development of phase field models. Occasionally, phase field models do help in formulating new theoretical models.

3.1 Some basics of thermodynamics and mechanics

As noted, starting from Gibbs, there have been continuous attempts to understand the thermodynamics of stressed solids; the theories are obviously based on the notions of elastic energy, the minimization of free energy, and interfacial energy (since, in general, during the minimization of elastic energy, it is the interfacial energy that tends to increase); in addition, in cases where the understanding of kinetics is attempted, the notion of chemical potential also becomes important.[124]

There are two broad approaches taken in the literature; one is based on the classical variational approach—used by Gibbs and Grinfeld and extended by Larche and Cahn; and, the other is based on the concept of generalised forces (called accretive forces or configurational forces)—used by Eshelby[125,126] and others: see for example.[127–132] In this review, we will primarily focus on the variational approach (though the widespread use of Eshelby energy-momentum tensor is common even in variational approach and is described in the next section). We refer the interested reader to the monographs of Maugin[133] and Gurtin[134] for detailed exposition of configurational force based formulations.

Norris,[124] in a very nice exposition on the notion of chemical potential in elastically stressed solids (based on[122,135–141]), has drawn attention to several important and subtle ideas and notions that need very careful consideration. They can be summarised as follows:

- As noted in the ATG instability case above, in all of elastic stress induced microstructural instabilities, we have to consider two cases: one in which diffusional processes redistribute existing material (denoted as static by us) and the other in which material is transferred from the surrounding (denoted as dynamic by us);
- In continuum mechanics, usually, there are two approaches that are taken to define quantities of interest, namely, the Lagrangian or material coordinate and, the Eulerian or current coordinate. The expressions for chemical potential in these two approaches, though formally equivalent, are not symmetric, and hence are to be used with care;
- The distinction in the coordinate frames for description can also be taken further; there are two surface energy descriptions, namely, Herring (based on Lagrangian) and Laplace (based on Eulerian); and,
- If a variational approach is taken to the minimization of energy, then, in the case of (crystalline) solids, allowed variations are to be defined with great care.

The papers on the thermodynamics of stressed solids are huge in number: see for example.[142–153] However, as seen in some of these recent attempts[154–156] the quest for the formulation of thermodynamically consistent phase field models that obey relevant principles and laws of mechanics is far from complete.

3.2 *Eshelby energy-momentum tensor*

Eshelby introduced the notion of elastic energy-momentum tensor[126] defined as follows:

$$P = W1 - \nabla u^T \sigma \qquad (1)$$

where W is the strain energy density, $\boldsymbol{\sigma}$ is the stress and $\boldsymbol{u}$ is the displacement. The integral of the normal component of the energy-momentum tensor over a surface gives the force acting on the defects and inhomogeneities enclosed by the surface. The introduction of such a force (called accretive or configurational force, as noted above) acting on a defect or inhomogeneity in an elastic continuum is very useful; once such a force is known, the change in elastic potential due to the size and shape changes of the defect (as in rafting and ATG instabilities, for example) can be calculated, as we discuss below.

Configurational force: force acting on defects and inhomogeneities in an elastic continuum.

3.3 *Equivalent eigenstrain and homogenisation problem*

The elastic inhomogeneity plays a key role in some of the elastic stress induced instabilities; for example, for both ATG instability and rafting, elastic instability is necessary; in elastically homogeneous systems, there will be neither rafting nor ATG instability. Further, the elastic inhomogeneity can lead to surprising results as in the case of coherent spinodal discussed below. When it comes to dealing with elastically inhomogeneous systems, there are two approaches. In the first one, pioneered by Eshelby, the inhomogeneous problem is replaced by a homogeneous problem by defining an equivalent eigenstrain. On the other hand, the approach taken in the composites literature is to come up with a homogeneous effective moduli of the two phase mixture. As we see below, while the method of equivalent eigenstrain is useful in deriving analytical solutions, the majority of phase field models that we will describe in this review are based on the idea of homogenisation.

Eigenstrain: stress-free strain such as thermal and transformational strain.

3.4 *Equation of mechanical equilbrium*

As noted above, elastic inhomogeneity in systems with coherency driven eigenstrains and imposed strains or applied tractions is the key problem in elastic stress driven microstructural instabilities. Thus, obtaining the stress and strain fields in such systems is at the heart of the phase field models. The stress and strain fields are obtained by solving the equation of mechanical equilibrium, namely,

$$\nabla \cdot \boldsymbol{\sigma}^{el} = \frac{\partial \sigma_{ij}^{el}}{\partial r_j} = 0 \quad in \ \Omega. \qquad (2)$$

where $\boldsymbol{\sigma}^{el}$ is the elastic stress.

Let the computational domain consists of two phases, namely, a matrix (m) and a precipitate (p). Let us assume that both the m and p phases are Hookean (that is, linearly elastic):

$$\boldsymbol{\sigma}_{kl}^{el} = C_{ijkl}\varepsilon_{ij}^{el}, \qquad (3)$$

where ε^{el} be the elastic strain and C_{ijkl} is the composition (and hence, position) dependent elastic modulus tensor; that is, the solid is elastically inhomogeneous.

The elastic strain is derivable from the total strain ε:

$$\varepsilon_{ij}^{el} = \varepsilon_{ij} - \varepsilon_{ij}^{0}, \qquad (4)$$

with ε^0 being the position dependent eigenstrain (misfit strain) tensor field. The total strain ε_{ij} is compatible; that is, it is derivable from the displacement field u as follows:

$$\varepsilon_{ij} = \frac{1}{2}(\nabla u + \nabla u^T) = \frac{1}{2}\left\{\frac{\partial u_i}{\partial r_j} + \frac{\partial u_j}{\partial r_i}\right\}. \qquad (5)$$

Using the symmetry properties of the moduli tensor, the equation of mechanical equilibrium can be written as:

$$\frac{\partial}{\partial r_j}\left(C_{ijkl}\frac{\partial u_i}{\partial r_k} - \varepsilon_{jl}^0\right) = 0 \quad in \ \Omega. \qquad (6)$$

In this partial differential equation, the coefficients are composition (and hence position) dependent. Such partial differential equations with varying coefficients require the technique of homogenisation for their solution.[157,158] In the next section, we discuss the homogenisation technique.

3.5 *Homogenisation*

Let us assume the following composition dependence:

$$\varepsilon_{ij}^0(c) = \beta(c)\varepsilon^T \delta_{ij}, \qquad (7)$$

where, ε^T is a constant that determines the strength of the eigenstrain, δ_{ij} is the Kronecker delta, and $\beta(c)$ is a scalar function of composition; and,

$$C_{ijkl}(c) = C_{ijkl}^{eff} + \alpha(c)\Delta C_{ijkl}, \qquad (8)$$

where $\alpha(c)$ is a scalar function of composition, and,

$$\Delta C_{ijkl} = C_{ijkl}^p - C_{ijkl}^m \qquad (9)$$

where, C_{ijkl}^p and C_{ijkl}^m are the elastic moduli tensor of the p and m phases respectively, and C_{ijkl}^{eff} is an "effective" modulus.

With these composition dependence for the eigenstrains and elastic moduli, we want to solve the Eq. 6. The computational domain is assumed to be a representative volume element; that is, we will assume the composition field to be periodic on the domain. This implies that some of the fields that are derived from composition such as eigenstrains and elastic moduli are also periodic; on the other hand, applied tractions will have to be anti-periodic. Thus, Eq. 6 has to be solved with such periodic and anti-periodic boundary conditions. In addition, there are also boundary conditions of either applied traction or imposed strains. The imposition of these boundary conditions is achieved using 'homogenisation': that is, we define the mean strain and stress in the computational domain as follows:

$$\langle \{\varepsilon_{ij}\} \rangle = E_{ij}, \tag{10}$$

where ε is the total strain, and the symbol $\{\cdot\}$ is defined as follows:

$$\langle \{\cdot\} \rangle = \frac{1}{V} \int_{\Omega} \{\cdot\} d\Omega, \tag{11}$$

where V is the volume of the representative domain Ω; and,

$$\langle \{\sigma_{ij}^{el}\} \rangle = \frac{1}{V} \int_{\Omega} \sigma_{ij}^{el} d\Omega. \tag{12}$$

The mean stress thus calculated should equal the applied stress σ^A.[40,159,160] This conclusion namely, that the mean stress should equal the applied stress, is arrived at using homogenisation assumption by some authors[159,160] while Jin et al.[40] used a variational approach.

The Eq. (8) is written assuming that in spite of the inhomogeneities at the microscopic scale, the domain Ω behaves as if it is a single homogeneous block with an "effective" elastic modulus C_{ijkl}^{eff}; the local microscopic perturbations in the elastic moduli (with respect to C_{ijkl}^{eff}) are described using the difference between the elastic constants of the p and m phases (ΔC_{ijkl}). As noted, the relevant boundary conditions are imposed strains or applied traction; since we will be using a spectral technique, we assume that the domain is periodic; hence, if macroscopic system is subjected to a homogeneous stress state σ^A, then, the applied traction on the boundaries of the domain Ω will

be anti-periodic; i.e., $\boldsymbol{\sigma} \cdot \mathbf{n}$, is opposite on opposite sides of $\partial \Omega$ with $\mathbf{n}$ being the unit normal to the boundary.[159,160]

The definition of periodic strain is again a result of homogenisation. By the imposed periodic boundary condition, the solution to the equilibrium equation (Eqn. (2)) will be such that the strain field $\varepsilon(\mathbf{r})$ is periodic on Ω. However, we have posed the equation of mechanical equilibrium in terms of the displacement field. Since the strains are derived from displacements by differentiation, the displacement field $\mathbf{u}(\mathbf{r})$, which gives rise to such periodic strain fields can always be written as follows:[159]

$$\mathbf{u} = \mathbf{E} \cdot \mathbf{r} + \mathbf{u}^\star, \tag{13}$$

where, $\mathbf{u}^\star$ is a displacement field that is periodic on Ω and $\mathbf{E}$ is a constant, homogeneous strain tensor. $\mathbf{E}$ can be assumed to be symmetric (without loss of generality) since the antisymmetric part corresponds to a rigid rotation of the cell. The 'homogenisation' implies[159] that $\mathbf{E}$ is the mean strain tensor of the cell (see Appendix D in[161]).

Let $\varepsilon^\star$ be the periodic strain; then, the strain we derive from the displacement equation (13) becomes (see Appendix D in[161]),

$$\varepsilon_{ij} = E_{ij} + \varepsilon_{ij}^\star, \tag{14}$$

where,

$$\varepsilon_{ij}^\star = \frac{1}{2}\left\{ \frac{\partial u_i^\star}{\partial r_j} + \frac{\partial u_j^\star}{\partial r_i} \right\}, \tag{15}$$

and the equation of mechanical equilibrium (2) is

$$\frac{\partial}{\partial r_j}\{C_{ijkl}(E_{kl} + \varepsilon_{kl}^\star - \varepsilon_{kl}^0)\} = 0. \tag{16}$$

Using the mean stress equation, it is easy to show that

$$E_{ij} = S_{ijkl}\left(\sigma_{kl}^A + \langle \{\sigma_{kl}^0\} \rangle - \langle \{\sigma_{kl}^\star\} \rangle \right). \tag{17}$$

where,

$$S_{ijkl} = \left(\langle \{C_{ijkl}\} \rangle \right)^{-1}, \langle \{\sigma_{ij}^\star\} \rangle = \langle \{C_{ijkl}\varepsilon_{kl}^\star\} \rangle, \\ \text{and } \langle \{\sigma_{ij}^0\} \rangle = \langle \{C_{ijkl}\varepsilon_{kl}^0\} \rangle. \tag{18}$$

and, ε^0 is the composition (and hence) dependent eigenstrain and $\varepsilon^\star$ is the periodic strain.

So, we obtain

$$\sigma_{ij}^A = \frac{1}{V}\int_\Omega C_{ijkl}(E_{kl} + \varepsilon_{kl}^\star - \varepsilon_{kl}^0)d\Omega. \tag{19}$$

Thus, using homogenisation, the equation of mechanical equilibrium can be restated as follows:

Given a periodic composition field c on Ω, solve the **equation of mechanical equilibrium**

$$\frac{\partial}{\partial r_j}\{C_{ijkl}(E_{kl} + \varepsilon_{kl}^\star - \varepsilon_{kl}^0)\} = 0 \text{ on } \Omega, \tag{20}$$

with the **constraint**

$$E_{ij} = S_{ijkl}\left(\sigma_{kl}^A + \langle\{\sigma_{kl}^0\}\rangle - \langle\{\sigma_{kl}^\star\}\rangle\right) \tag{21}$$

and the **boundary condition**

$$\varepsilon_{kl}^\star \text{ is periodic on } \Omega. \tag{22}$$

In this formulation, now it is easy to implement an overall prescribed strain ($E_{ij} \neq 0$). It is also possible to prescribe overall stress using the same quantity; this approach of stress control is known as "stress-control based on strain-control" and is described in.[160]

Substituting for C_{ijkl}, and ε_{kl}^0 in terms of composition, and $\varepsilon_{kl}^\star$ in terms of the displacement field in Eqn. (20), and using the symmetry properties of the elastic constants and strains, we obtain

$$\frac{\partial}{\partial r_j}\left\{\left[C_{ijkl}^{eff} + \alpha(c)\Delta C_{ijkl}\right]\left(E_{kl} + \frac{\partial u_l^\star(\mathbf{r})}{\partial r_k} - \varepsilon^T\delta_{kl}\beta(c)\right)\right\} = 0. \tag{23}$$

$$\left[C_{ijkl}^{eff}\frac{\partial^2}{\partial r_j \partial r_k} + \Delta C_{ijkl}\frac{\partial}{\partial r_j}\left(\alpha(c)\frac{\partial}{\partial r_k}\right)\right]u_l^\star(\mathbf{r})$$

$$= C_{ijkl}^{eff}\varepsilon^T\delta_{kl}\frac{\partial\beta(c)}{\partial r_j} - \Delta C_{ijkl}E_{kl}\frac{\partial\alpha(c)}{\partial r_j}$$

$$+ \Delta C_{ijkl}\varepsilon^T\delta_{kl}\frac{\partial\{\alpha(c)\beta(c)\}}{\partial r_j}. \tag{24}$$

3.6 *Fourier transform based iterative solution to the equation of mechanical equilibrium*

The equation of mechanical equilibrium is typically solved using finite element technique. However, the finite element method requires meshing of the domain with denser mesh close to the interfaces. In phase field models, this cost of meshing can be too high; for example, in a system undergoing spinodal decomposition, the entire domain, at least in the early stages of decomposition, consists only of interfaces (albeit at various stages of formation). In addition, as the microstructure evolves the interfaces continuously merge and split, and new interfaces appear while old ones disappear. Hence, in the phase field literature, an alternate iterative method based on spectral techniques is widely used for solving the equation of mechanical equilibrium; in this section, we describe the method. The disadvantage with this method, is, of course that it is iterative (though there are methods proposed, based on FFT to tackle these situations also: see[162]). So, when the 'contrast' (that is, the ratio of elastic moduli of the two phases) is too high, the iterations take much longer to converge making finite element implementations (which solve the problem in one step) competitive. The spectral techniques are based on Fourier transform; hence the use of numerically efficient Fast Fourier Transform codes (such as FFTW[163]) is widespread in the implementations of this method.

The iterative technique for solving the equation of mechanical equilibrium using Fourier transforms is well known:[40,159,160,164–168] our description below is based on.[161] Since we are using the Fourier transform based technique, in the computational domain Ω the fields are either periodic (for example, the composition, and the moduli and eigenstrains that follow the composition) or anti-periodic (for example, the applied traction). As noted in the previous section, the assumption of periodicity of computational domain is also justified physically since the domain is the representative volume element.

3.6.1 Zeroth order approximation: Assume $\Delta C_{ijkl} = 0$; the equation of mechanical equilibrium (2) simplifies to

$$C_{ijkl}^{eff}\frac{\partial^2 u_l^\star(\mathbf{r})}{\partial r_j \partial r_k} = C_{ijkl}^{eff}\varepsilon^T\delta_{kl}\frac{\partial\beta(c)}{\partial r_j}. \tag{25}$$

Let $\sigma_{ij}^T = C_{ijkl}^{eff}\varepsilon^T\delta_{kl}$:

$$C_{ijkl}^{eff}\frac{\partial^2 u_l^\star(\mathbf{r})}{\partial r_j \partial r_k} = \sigma_{ij}^T\frac{\partial\beta(c)}{\partial r_j}. \tag{26}$$

Let G_{il}^{-1} as $C_{ijkl}g_jg_k$ (where $\mathbf{g}$ is the vector in the Fourier space). Then the solution (in the Fourier space) for the equation above is[161]

$$\left\{(u_l^\star)^0\right\}_\mathbf{g} = -JG_{il}\sigma_{ij}^T g_j\{\beta(c)\}_\mathbf{g}, \tag{27}$$

where the superscript on $u_k^\star$ denotes the order of approximation, and J is $\sqrt{(-1)}$.

3.6.2 Higher order approximations: The zeroth order approximation can be refined to obtain the first order solution. This process can be continued to higher orders; knowing the $(n-1)$th order solution, the nth order refined solution as follows:

$$\{(u_l^\star)^n\}_\mathbf{g} = -J G_{il} \Lambda_{ij}^{n-1} g_j, \qquad (28)$$

where

$$\Lambda_{ij}^{n-1} = \sigma_{ij}^T \{\beta(c)\}_\mathbf{g} - \Delta C_{ijmn} E_{mn}^{n-1} \{\alpha(c)\}_\mathbf{g}$$
$$+ \Delta C_{ijmn} \varepsilon^T \delta_{mn} \{\alpha[c(\mathbf{r})] \beta[c(\mathbf{r})]\}_\mathbf{g}$$
$$- \Delta C_{ijmn} \left\{ \alpha[c(\mathbf{r})] \frac{\partial (u_m^\star)^{n-1}(\mathbf{r})}{\partial r_n} \right\}_\mathbf{g} \qquad (29)$$

3.7 Spinodal phase separation: Suppression and promotion

The elastic field induced suppression of spinodal decomposition is very well known.[169] However, that elastic strains can promote spinodal decomposition is not widely recognized.[51] In this section, we describe the analyses of both these scenarios. Unlike the other theoretical studies described in this section (which are sharp interface models), the description of spinodal decomposition necessarily involves building a phase field model. So, we describe the classical (sharp interface model of) diffusion before discussing the models of spinodal decomposition.

3.7.1 Classical diffusion equation and its failure: Let us consider the classical diffusion equation: it is based on the constitutive law (known as Fick's first law), which connects the atomic flux (denoted by $\mathbf{J}$) to concentration gradient (∇c) through the material property known as diffusivity tensor ($\mathbf{D}$):

$$\mathbf{J} = -\mathbf{D}\nabla c \qquad (30)$$

The diffusivity is a second rank tensor; hence, in isotropic and cubic systems it is replaced by $D\delta_{ij}$ where δ_{ij} is the Kronecker delta and D is a material constant known as diffusion coefficient. For the rest of this review, we use diffusion coefficient.

Using the law of conservation of mass in differential form,

$$\frac{\partial c}{\partial t} = -\nabla \cdot J \qquad (31)$$

along with Fick's first law, one obtains the classical diffusion equation (which is also called Fick's second law):

$$\frac{\partial c}{\partial t} = \nabla \cdot D\nabla c \qquad (32)$$

If the diffusivity is assumed to be a constant (that is, not a function of composition, and hence, position), we obtain

$$\frac{\partial c}{\partial t} = D\nabla^2 c \qquad (33)$$

This equation indicates that the rate of change of composition at any point is given by the curvature of the composition profile at that point; hence, if one assumes a sinusoidal composition profile, one can see that the compositional heterogeneities will be evened out with time. However, in some systems, it was known that compositional heterogeneities grow with time (leading to phase separation—called spinodal decomposition) instead of getting evened out, giving rise to the so-called "up-hill" diffusion.

One way that the compositional heterogeneities will grow if the diffusivity is a negative constant. The negative value of diffusion coefficient can be explained if the Fick's first law is modified using the knowledge of classical thermodynamics, namely, that it is the chemical potential gradients that drive diffusion and not compositional heterogeneities. In other words, the modified Fick's first law states that

$$\mathbf{J} = -M\nabla\mu \qquad (34)$$

where M is the mobility tensor and μ is the chemical potential, defined as $\frac{\partial(G/N_v)}{\partial c}$ where G/N_V is the Gibbs free energy per atom (N_V is the number of atoms per mole, and G is the Gibbs free energy per mole). Here again, in isotropic and cubic systems M can be replaced by $M\delta_{ij}$ where M is the mobility; for the rest of this review, we use M and not the mobility tensor. Note that in condensed systems, the Gibbs and Helmholtz free energies can be assumed to be the same.

Combining this constitutive law with the law of conservation of mass, one obtains

$$\frac{\partial c}{\partial t} = \nabla M \nabla \mu \qquad (35)$$

If we assume the mobility to be a constant independent of composition, one can see that the mobility and diffusivity are related through the relationship:

$$D = M \nabla^2 (G / N_V) \qquad (36)$$

In other words, when the sign of the curvature of the free energy versus composition curve is negative, one expects the diffusivity to become negative and the up-hill diffusion to take place and the classical diffusion takes place when the curvature of the free energy versus composition curve is positive. Thus, the point where the curvature of the free energy versus composition curve becomes zero, (that is, $G'' = \frac{\partial^2 G}{\partial c^2} = 0$) defines the region in which spinodal decomposition will take place.

3.7.2 Going beyond classical diffusion equation: The chemical potential based constitutive law can (partially) explain spinodal phase separation—namely, it can explain the 'up-hill' diffusion. However, it does not explain all the observed phenomena. Specifically, if the diffusivity is negative, one expects sinusoidal composition profiles of any wavelength to grow with time; further, smaller the wavelength, faster will be the growth of such composition waves (since shorter diffusion distances lead to smaller diffusion times). However, in such up-hill diffusion cases, it is known that only compositional heterogeneities with a wavelength greater than certain critical wavelength grow,[169] and the amplitude of any wavelengths shorter than the critical wavelength diminishes with time.

Cahn[170] showed that the critical wavelength is a consequence of the (incipient) interface energy (due to the formation of the two phases). As we discuss in the next section, incorporation of this interfacial contribution through a (positive) constant known as the gradient energy coefficient (K) leads to a modified diffusion equation (in 1-D):

$$\frac{\partial c}{\partial t} = \left(\frac{M}{N_V}\right)\left[G'' \frac{\partial^2 c}{\partial x^2} - 2K \frac{\partial^4 c}{\partial x^4}\right] \qquad (37)$$

Further, in solids, if the two phases are coherent, the phase separation can also lead to eigenstrains. Let η be the strength of the eigenstrain (ε^T), where η is the Vegard's coefficient:

$$\eta = \frac{1}{a_0} \frac{da}{dc}\Big|_{c=c_0}, \qquad (38)$$

Up-hill diffusion: diffusion which enhances compositional gradients.

where, c_0 is the overall alloy composition, a and a_0 are the composition dependent lattice parameter and the lattice parameter of the reference (i.e., of the homogeneous alloy) respectively. In such elastically stressed systems, Cahn[121,170–173] showed that elastic strains can suppress spinodal decomposition, leading to the description of what is known as coherent spinodal, which has now become standard textbook material.[174]

To understand coherent spinodal, let us consider the modified diffusion equation of Cahn in 1-D (including elastic strain):[169]

$$\frac{\partial c}{\partial t} = \left(\frac{M}{N_V}\right)\left[(G'' + 2\eta^2 Y)\frac{d^2 c}{dx^2} - 2K \frac{d^4 c}{dx^4}\right]. \qquad (39)$$

Consider a spatial composition profile described by

$$c - c_0 = \int A(\beta)\exp(i\beta x)d\beta \qquad (40)$$

where c_0 is the overall alloy composition and β is the wavenumber (related to the wavelength λ as $2\pi/\lambda$). If we substitute this profile in Eq. 39, we obtain the differential equation:

$$\frac{dA}{dt} = -\left(\frac{M}{N_V}\right)\left[G'' + 2\eta^2 Y + 2K\beta^2\right]A\beta^2 \qquad (41)$$

The solution of this differential equation is:

$$A(\beta,t) = A(\beta,0)\exp(R(\beta)t) \qquad (42)$$

where $R(\beta) = -(\frac{M}{N_V})[G'' + 2\eta^2 Y + 2K\beta^2]\beta^2$. From this solution, it is clear that the sign of $R(\beta)$ determines whether a given composition profile will grow or not.

Let us first consider the case where there is no eigenstrain ($\eta = 0$). If $G'' > 0$, the composition fluctuations die out irrespective of β. However, if $G'' < 0$, there is a critical wavenumber $\beta_c = \sqrt{\frac{-G''}{2K}}$ (obtained by equating $[G'' + 2K\beta^2]$ to zero). Any wavenumber smaller than this will grow and any wavenumber larger than this will grow. The point at which $G'' = 0$ is known as the (chemical) spinodal. Let us now assume $\eta \neq 0$. In this case, the critical wavenumber is given by $\beta_c = \sqrt{\frac{-G'' - 2\eta^2 Y}{2K}}$. Hence, the point at which $G'' + 2\eta^2 Y = 0$ is known as coherent spinodal. Since $Y\eta^2$ is a positive quantity, it is clear that the elastic stresses suppress spinodal decomposition.

3.8 Stability analysis in an elastically inhomogeneous system under imposed strains

The iterative procedure described above (in Sec. 6) can be used to obtain (approximate) analytical solutions in certain elastically inhomogeneous systems; for example, in a system with a sinusoidal composition profile under plane stress approximation. Obtaining such an analytical solution helps us extend the spinodal analysis of Cahn.

Let us assume the following composition dependence for the α and γ functions, namely, the composition dependence of the elastic moduli and eigenstrain (described in Sec. 5), respectively:

$$\alpha(c) = \gamma(c) = c - c_0 \tag{43}$$

Note that in this part of the derivation we have used γ for the composition dependence of eigenstrain (instead of β as earlier) to avoid confusion with the wavenumber denoted by β.

3.8.1 Zeroth order approximation: The solution to Eq. (6) assuming a homogeneous modulus, in Fourier space is given by[168] (as shown in Eq. 1):

$$\{(u_l^*)^0\}_g = -JG_{li}\sigma_{ij}^T\{\gamma(c)\}_g g_j, \tag{44}$$

where, $G_{il}^{-1} = C_{ijkl}^{eff}g_jg_k$ and $\sigma_{ij}^T = C_{ijkl}^{eff}\eta\delta_{kl}$; $\{\cdot\}_g$ denotes the quantity inside brackets to be in Fourier space; g_j denotes the jth component of the Fourier space vector $\mathbf{g}$.

By adopting a similar approach to Cahn's,[170] we assume, $c - c_0 = A\cos\beta x$, where $2\pi/\beta$ represents any generic wavelength. So, in Fourier space, we get:

$$\begin{bmatrix} (u_1^*)^0 \\ (u_2^*)^0 \end{bmatrix}_g = \begin{bmatrix} \dfrac{\eta(1+\nu)}{\beta}A\pi J[\delta(g+\beta)-\delta(g-\beta)] \\ 0 \end{bmatrix}, \tag{45}$$

which when reverted back to the real space, we get:

$$\begin{bmatrix} (u_1^*)^0 \\ (u_2^*)^0 \end{bmatrix}_r = \begin{bmatrix} \dfrac{\eta(1+\nu)}{\beta}A\sin\beta x \\ 0 \end{bmatrix}. \tag{46}$$

Thus the only non-zero periodic strain component is:

$$(\epsilon_{11}^*)^0 = \eta(1+\nu)A\cos\beta x = \eta(1+\nu)(c-c_0). \tag{47}$$

3.8.2 First order approximation: As we are interested in deriving expressions valid for very early stages, we can neglect the non-linear terms in the expression given in Ref.[168] Thus the expression for the periodic displacement field becomes:

$$\begin{aligned}\{(u_l^*)^1\}_g &= -JG_{li}\sigma_{ij}^T\{\gamma(c)\}_g g_j \\ &+ JG_{li}\Delta C_{ijmn}E_{mn}^0\{\alpha(c)\}_g g_j,\end{aligned} \tag{48}$$

where, $E_{mn} = e\delta_{mn}$, with the reference being the unstrained homogeneous alloy lattice. The first term in the right hand side (RHS) of Eq. (48) is the solution to the zeroth order approximation which we already have in Eq. (45). So, we are going to consider only the second term in the RHS of Eq. (48). Denoting it by v, we get:

$$\begin{bmatrix} v_1^* \\ v_2^* \end{bmatrix}_g = \begin{bmatrix} -\dfrac{ye(1+\nu)}{\beta}A\pi J[\delta(g+\beta)-\delta(g-\beta)] \\ 0 \end{bmatrix}, \tag{49}$$

where y is given as:

$$y = \frac{1}{Y_0}\frac{dY}{dc}\bigg|_{c_0} = \frac{\Delta Y}{Y_0}, \tag{50}$$

with Y_0 denoting the Young's modulus of the homogeneous alloy and $\Delta Y = Y^p - Y^m$. In the real space:

$$\begin{bmatrix} v_1^* \\ v_2^* \end{bmatrix}_r = \begin{bmatrix} -\dfrac{ye(1+\nu)}{\beta}A\sin\beta x \\ 0 \end{bmatrix}. \tag{51}$$

So the periodic diplacement field obtained from the First order approximation is given by:

$$\begin{bmatrix} (u_1^*)^1 \\ (u_2^*)^1 \end{bmatrix}_r = \begin{bmatrix} (u_1^*)^0 + v_1^* \\ (u_2^*)^0 + v_2^* \end{bmatrix}_r = \begin{bmatrix} \dfrac{(\eta-ye)(1+\nu)}{\beta}A\sin\beta x \\ 0 \end{bmatrix}. \tag{52}$$

The periodic strain field is given by,

$$\begin{aligned}(\epsilon_{11}^*)^1 &= (\eta-ye)(1+\nu)A\cos\beta x \\ &= (\eta-ye)(1+\nu)(c-c_0),\end{aligned} \tag{53}$$

with the other strain components being zero.

3.8.3 Elastic Energy: The total strain energy is given by:

$$F_{el} = \frac{1}{2}\int_\Omega \sigma_{ij}^{el}\epsilon_{ij}^{el}\,d\Omega, \tag{54}$$

Substituting for the elastic modulus tensor components in terms of Y and v and setting $\epsilon_{11}^* = P(c - c_0)$ where $P = \eta(1 + v)$ for zeroth order approximation and $P = (\eta - ye)(1 + v)$ for first order approximation respectively, we get:

$$W_E = \frac{1}{2} \int_\Omega \left[\frac{Y_0}{1 - v^2} P^2 - \frac{2Y_0(1 + v)}{1 - v^2} \eta P + \frac{2Y_0(1 + v)}{1 - v^2} \eta^2 \right.$$
$$\left. + \frac{2\Delta Y(1 + v)}{1 - v^2} eP - \frac{4\Delta Y(1 + v)}{1 - v^2} e\eta \right] (c - c_0)^2 d\Omega.$$

(55)

where we have neglected the constant terms as they do not contribute to the elastic chemical potential. Proceeding as in Ref.,[170] we get the expression for the maximally growing wave-number for the zeroth order approximation as:

$$\beta_{max} = \left[-\frac{\left(\frac{\partial^2 f_0}{\partial c^2} + \eta^2 \frac{Y_0}{N_V} \left(1 - \frac{2ey}{\eta} \right) \right)}{4K} \right]^{\frac{1}{2}},$$

(56)

while for the first order approximation, we get:

$$\beta_{max} = \left[-\frac{\left(\frac{\partial^2 f_0}{\partial c^2} + \eta^2 \frac{Y_0}{N_V} \left(1 - \frac{2ey}{\eta} \right) - \frac{Y_0(1 + v)^2 y^2 e^2}{N_V(1 - v^2)} \right)}{4K} \right]^{\frac{1}{2}}.$$

(57)

The zeroth order approximation given by Eq. (56) has the following salient features:

1. On setting $\eta = 0$, we recover Cahn's results[170] for a system with no elastic misfit.
2. Cahn's expression of the maximally growing wavenumber[170] for a system with a non-zero η (but the elastic modulus tensor being a constant) is recovered by setting either $y = 0$ or $e = 0$. Thus, there is no influence of a non-zero y when $e = 0$, and vice versa.
3. When $2ey/\eta > 0$, the positive contribution from the elastic energy goes down, which manifests as larger maximally growing wavenumbers (i.e., shorter wavelengths) compared to that predicted by Cahn's theory for a system with homogeneous modulus.

Compared to Eq. (56) Eq. (57) has an additional term. This new term (let this be called A) is:

$$A = -\frac{Y_0(1 + v)^2 y^2 e^2}{N_V(1 - v^2)}.$$

(58)

This new term has the following features:

1. There is no η in Eq. (69). So, its contribution is independent of the value of the misfit in the system.
2. The energy contribution is negative regardless of the signs of e or y. Thus, for given values of e and y, from the first order approximation we get a β_{max}, which is larger than that obtained from the zeroth order approximation. In other words, this term promotes phase separation.

We will use these expressions in the next section to show how the imposed strains in these systems can promote spinodal decomposition even outside of chemical spinodal.

3.9 *Particle splitting*

The particle splitting instability is attributed to elastic interaction energy[66,69,175–177] between the misfitting precipitates; that is, for a given volume, if there are more than one precipitate aligned along certain directions of the matrix, the interaction energy between such misfitting precipitates is predicted to lead to a reduction in energy which more than compensates for the increase in interfacial energy during splitting. However, this is not the only explanation. As we discuss in the next section, phase field models have shown that nucleation at dislocations, anti-phase domains of ordered precipitates, growth instabilities, particle coalescence, and, applied stress can also lead to split patterns. Thus, currently, the theoretical analysis of this instability is neither complete nor comprehensive.

3.10 *Rafting*

One of the earliest studies on rafting considering elastic stresses is due to Pineau.[178] The study of precipitate shape evolution and symmetry breaking transitions of Johnson and Cahn[123] is another pioneering early study on the effect of elastic stresses on particle morphologies. Following these, there have also been several studies on the shape evolution and stability of precipitates under applied stresses considering single[179–181] and multiparticle[182,183] scenarios.

One of the difficulties with these analytical studies is the evaluation of elastic field for arbitrary shapes of precipitates and taking into consideration the elastic moduli differences.

However, based on these analytical studies, it was shown that the driving force for rafting is proportional to (i) the elastic moduli mismatch; (ii) the misfit; and (iii) the applied stress (when the elastic moduli mismatch is small). In fact, the sign of rafting, namely, if the precipitates coarsen perpendicular (called N-type rafting) or parallel (called P-type rafting) to applied uniaxial stress depends on the signs of these three quantities. Let δ be the ratio of the shear modulus of the precipitate to that of the matrix. Then, P (N) type rafting occurs when $\sigma^A \varepsilon^0 (1 - \delta) < 0 (> 0)$ where σ^A is the applied stress (with tensile being positive) and ε^0 is the eigenstrain (which is assumed positive if the lattice parameter of the precipitate is larger than the precipitate) for small δ. Thus, changing the sign of any of these keeping the other two constant will switch the type of rafting. In addition, the differences in anisotropy and the Poisson's ratio of the two phases as well as large deviations of δ from unity has a strong say on rafting;[184] however, in those cases the above rule breaks down.

Note that most of the analytical studies of rafting assume Hookean elasticity and are based on thermodynamic considerations—either by considering the elastic energies associated with different shapes of coherent precipitates or by considering the chemical potential contours surrounding a misfitting precipitate.

The most complete analysis of the rafting problem (assuming purely elastic stresses) is due to Schmidt and Gross.[184] Schmidt and Gross consider the instantaneous chemical potential at different points of a given precipitate and use it to predict rafting behaviour. Here we summarise the approach of Schmidt and Gross by highlighting the key steps and the results: the algebra is fairly detailed and we refer the interested reader to.[184]

- Consider a two phase material with a coherent, misfitting precipitates in a matrix, assuming both the matrix and precipitate phases to be Hookean elastic. The change in potential of the system (strain energy), δW^{el}, due to the migration of the matrix-precipitate interface by an amount δl in the direction n (normal to the precipitate-matrix interface into matrix from the precipitate) is calculated using the energy-momentum tensor of Eshelby:

$$\delta W^{el} = -\int \tau_n \delta l dA \qquad (59)$$

where $\tau_n = n \cdot [P] n$ is the driving force with $[P]$ is the jump in the Eshelby energy-momentum tensor.

- Using the traction and displacement continuity equations, and using Eshelby's classic result,[185] namely that the total strain inside an inclusion is related to eigenstrain linearly through Eshelby tensor (S), one can show that

$$\tau_n = \frac{1}{2} \epsilon^0 : \Xi : \epsilon^0 \qquad (60)$$

where Ξ is a fourth rank tensor, which is related to elastic moduli of the two phases as follows (as hence has the same symmetry as moduli tensor):

$$\Xi = ([C]S + C^p)^T \gamma(n)([C]S + C^p) - \Lambda \qquad (61)$$

where

$$\Lambda = C^p + C^p[C]C^p \qquad (62)$$

and

$$\Gamma(n) = [C]^{-1} - n \otimes \Omega^{-1}(n) \otimes n \qquad (63)$$

with $\otimes$ is the tensor product (outer product) and Ω is the acoustic tensor of the matrix: $\Omega_{ik} = C^m_{ijkl} n_j n_l$. Note that Ξ is only the function of elastic moduli and the shape of the precipitate.

- Consider the two phase system to be under an externally applied stress. Schmidt and Gross show that this problem is equivalent to the problem above (that is, without applied stress) albeit with a modified ("equivalent") eigenstrain ((ε^0)*):

$$(\epsilon^0)^\star = \epsilon^0 - [C^{-1}]\sigma^\infty \qquad (64)$$

where σ^∞ is the applied stress, can be defined; this idea is equivalent eigenstrain is very similar to that of Eshelby;[185] however, while Eshelby reduces the problem to one of homogeneous inclusion using his equivalent eigenstrain, in Schmidt and Gross's case, the inclusion remains inhomogeneous.

- Schmidt and Gross also manage to show that in case the precipitate volume remains constant and only shape changes, the driving force for the modified problem is the same as the original problem. These results are valid for more than one precipitate; it is independent of the geometry of the system; and, it is valid for arbitrary inclusion shapes.

- Once the equivalent inclusion is known, the problem can be solved using the Ξ tensor for

the modified eigenstrain. In case the precipitate volume fraction does not change, the modified τ_n calculated using the equivalent eigenstrain (and hence the modified Ξ) gives the change in potential.

- At this stage, to proceed further, it becomes necessary to assume some symmetry for the precipitate as well as their distribution, and calculate the change in potential for different elongations—as shown schematically. For a spontaneous process, the change in potential should be negative. Using this condition, maps of normalised applied stress and normalised elastic moduli ratio indicating the different regions of P or N type rafting are obtained (as shown in schematic).

3.11 *Asaro-Tiller-Grinfeld instabilities*

There are two approaches to the study of ATG instabilities; one is a perturbation analysis and the other is variational approach. While the variational approach results are stronger in the sense that the morphology that minimizes the free energy is identified using it, the perturbation analysis will give the morphology also taking into account the kinetics. There are morphological instabilities such as dendritic morphologies formed during solidification, which are a result of kinetics (how fast can the solidification front can move), and actually increase the interfacial free energy. Thus, both approaches
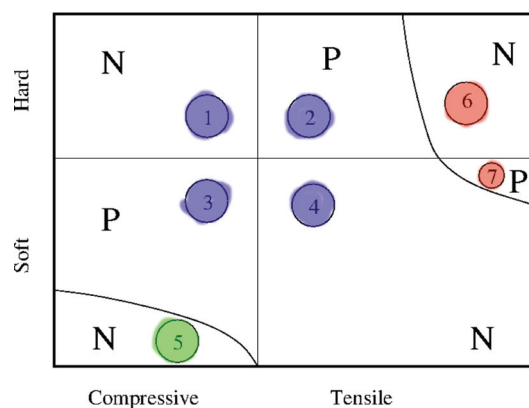
Figure 2: Schematic rafting behaviour based on the analysis of Schmidt and Gross, assuming a positive dilatational eigenstrain and an applied stress along the *x*-axis on particles with four-fold symmetry; the red regions (6 and 7) require the elastic anisotropy and Poisson's ratio of the two phases to be different; the green region (5) corresponds to $\delta \ll 1$; the blue regions (1, 2, 3, and 4) are where the P and N rule is valid. The figure is based on[184] and adapted from.[161]

are needed for a complete understanding of the morphological instabilities. In addition, since the ATG instabilities are of two types, namely, static and dynamic, while variational approaches are ideal for static studies, the perturbative approach can take the growth into account while analysing the stability.

There are a few relevant reviews/useful reviews/ that valid reviews discuss the elastic stress effects, from the point of view of applications, on surface instabilities,[186] on semiconductor heteroepitaxy[107] and epitaxial growth,[187] during crystal growth by atomic and molecular beams,[188] and, on wrinkling of surfaces in soft materials.[21] The instability analysis itself is summarised in several articles for several different scenarios: see, for example.[96,97,189–213] These papers can be classified in many different ways; for example, they can be classified based on the phases involved as solid-solid (for example, multilayers of solids), solid-liquid (for example, minerals in contact with stressed solids) and solid-vapour (for example, elastic half-spaces, plates and thin films), the mechanism assumed (volume diffusion or surface diffusion or evaporation-condensation), the assumptions about the elastic properties (isotropic or orthotropic), the geometry they assume (cylindrical pore, spherical cavity, thin film and so on), the source of elastic strain (applied stresses, pressure in fluid, coherency strains, imposed strains due to epitaxy and so on), whether they consider linear or nonlinear effects, the approach they take, namely the perturbative approach of Asaro-Tiller or the variational approach of Grinfeld. In this section, for the same of completeness, we briefly summarise the steps involved in the perturbative (using solid-solid, thin film geometry example[202]) and variational (using solid-liquid, curved solid in contact with fluid geometry example[191]) approaches.

3.11.1 Variational approach: The variational approach pioneered by Gibbs, namely, extremising the relevant free energy functional, is used to study the stability of stressed solid in contact with the second, compliant phase (be it solid, liquid or vapour), is described in this section (with specific reference to stressed solid in contact with a fluid). As noted by Heidug,[191] by demanding that, at equilibrium, there should be no production of entropy, one can derive the condition of chemical equilibrium at the interface as a jump condition, as done by Lehner and Bataille.[214] This entropy production approach shows that the conditions derived using Gibbsian approach are generic

and are independent of the specific constitutive behaviour assumed for the bulk phases or the loading configuration that the solid is subjected to.

Let us consider the equilibrium of a solid-fluid system as shown in the schematic Fig. 3; the system is at constant temperature and is enclosed by rigid boundaries. The equilibrium of such a system is determined by the minimization of the (Helmholtz) free energy

$$\Psi = \int_{R_s+R_f} \psi dv + \int_{\Sigma} \hat{\psi} da \qquad (65)$$

where the first term is the bulk free energy integrated over the solid (R_s) and liquid (R_f) volumes (in the reference state at equilibrium) and the second term is integrated over the interface area; the minimization has to be carried out subject to the conservation of the solvent (denoted by D) and solute (denoted by S) mass:

$$\int_{R_s+R_f} \rho^S dv + \int_{\Sigma} \hat{\rho}^S da = \text{Constant} \qquad (66)$$

$$\int_{R_s+R_f} \rho^D dv + \int_{\Sigma} \hat{\rho}^D da = \text{Constant} \qquad (67)$$

Thus, the problem we are considering is one of constrained minimization. So, we introduce the (undetermined) Lagrange multipliers λ^S and λ^D corresponding to the two constraints, and write the new functional to be optimized as follows:

$$\Phi = \Psi + \lambda^S \left[\int_{R_s+R_f} \rho^S dv + \int_{\Sigma} \hat{\rho}^S da \right] + \lambda^D \left[\int_{R_s+R_f} \rho^D dv + \int_{\Sigma} \hat{\rho}^D da \right] \qquad (68)$$

The minimization is achieved when the first variation $\delta\Phi$ is zero and the second variation is positive. The first variation leads to local

Figure 3: Schematic of solid-liquid system in reference configuration; based on.[191]

equilibrium conditions—which, in this case, are as follows:

- The chemical potential for the solvent and the solute are uniform;
- In solid and the fluid, the relevant equations of mechanical equilibrium is satisfied; that is, solid supports non-hydrostatic stress and in fluids the stress state is hydrostatic;
- At the interface, force balance for stressed membranes is satisfied; namely, capillary equilibrium for solid-fluid interface is satisfied; and at the interface, the shear stresses in the solid are balanced by surface tension.

The key piece in this derivation is the identification appropriate allowed variations. Specifically, the allowed variations should be such that (i) there are no displacements at the system boundary (since we assumed it to be rigid); (ii) the displacements at the interface have no discontinuity; (iii) in the solid phase, their gradient is the same as the variation of the deformation gradient; (iv) the displacements at the interface, when decomposed into the normal and tangential components, give rise to tangential components that are compatible with the (Gaussian) surface parameters; and (v) the interface velocity and the rate of change of interface metric that it gives rise to are compatible.

The second variation gives the stability criterion; it can be shown that stability demands that (i) the stress on the solid at the interface should be hydrostatic and equal to fluid pressure; and (ii) either the Gibbs surface energy vanishes or that the interface is flat.[191] Thus, phase equilibrium at non-hydrostatically stressed, curved solid-fluid interfaces is not stable.

3.11.2 Perturbative approach: Let us consider a perturbation of the solid-solid interfaces as shown in Fig. 4 in an elastically stressed solid. The (sinusoidal) perturbed interface profile is described by $y_i = \pm[\frac{h}{2} + \delta\cos(kx)]$, where δ is the amplitude of perturbation of wavelength $\lambda (= \frac{2\pi}{k})$ where k is the wavenumber and h is the height of the film as shown in the figure. We assume $\delta k \ll 1$; that is, the interface profile is such that its slope is very small everywhere; this assumption is what makes the analysis perturbative.

Let μ_0 be the chemical potential of the interface when it is flat and let μ be the chemical potential along the interface when the interface is perturbed. Let γ be the (isotropic) interfacial energy. Then,
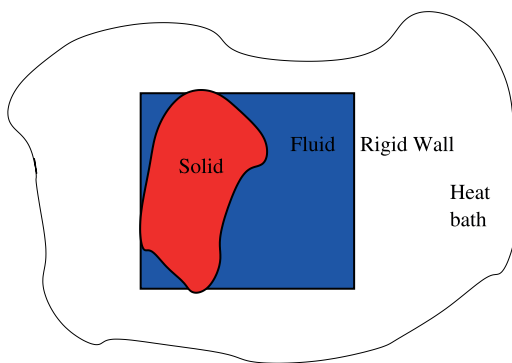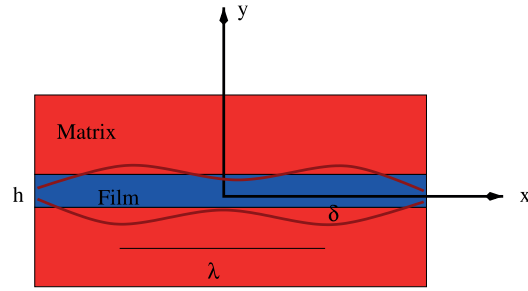
Figure 4: Schematic of perturbation of the film-matrix interface; based on.[202]

$$\mu - \mu_0 = \Omega\left(\kappa\gamma + [W]_-^+ - \mathbf{T}\cdot\left[\frac{\partial \mathbf{u}}{\partial n}\right]_-^+\right) \qquad (69)$$

where κ is the interface curvature; Ω is the atomic volume; $[W]_-^+$ is the jump in strain energy density across the interface; $\mathbf{T}$ is the traction on the interface; $\partial \mathbf{u}/\partial n$ is the derivative of the total displacement field in the direction normal to the interface. The first term on the RHS is due to interfacial energy; and, the last two terms on the RHS are due to elastic stresses and was derived by Eshelby using energy-momentum tensor.[126]

Thus, for the perturbed geometry, the equation of mechanical equilibrium is to be solved (under appropriate boundary conditions), and using the elastic solution obtained the second and third terms are to be evaluated. It is not possible to do this analytically. However, since we have assumed small slope for the interface everywhere, it is sufficient to obtain these quantities to first order in δk and such an approximate expression can be obtained—see these notes for the MAPLE™ script, which can be used to obtain the elastic solutions.[215] In addition, the interfacial curvature can also be shown, to first order in δk, to be $\delta k^2\cos(kx)$.

Let F be the force on atoms at the interface. It is relationship to the chemical potential is as follows: $F = -\frac{\partial \mu}{\partial s}$, where s is the distance along the interface (interfacial arc). By Fick's first law, the atomic flux is proportional to the force and the proportionality constant is the mobility M; that is, $J = MF$. The mobility is related to the diffusivity and interface width η through $M = D\eta/(\Omega k_B T)$, where k_B is the Boltzmann constant and T is the absolute temperature. Once the flux is given, using the conservation of mass, the velocity of the interface (ν) can be calculated as

$$\nu = -\Omega\frac{\partial J}{\partial s} = M\Omega\frac{\partial^2 \mu}{\partial s^2} \qquad (70)$$

However, the velocity can also be calculated to first approximation, by differentiating the interface profile with time, and hence.

$$\nu \approx \frac{\partial \delta}{\partial t}\cos(kx) = M\Omega\frac{\partial^2 \mu}{\partial s^2} \qquad (71)$$

The solution of this equation (since the RHS term can be shown to be sinusoidal) is

$$\delta(\tau) = \delta(0)\exp(\phi\tau) \qquad (72)$$

where both the time, τ and growth rate φ, are non-dimensional.

By solving the elastic problem under different boundary conditions and assuming different diffusion mechanisms, Sridhar et al.[202] showed that there are two possibilities of break-up for films—namely, symmetric and anti-symmetric. In fact, Sridhar et al.[202] give stability diagrams indicating the parameter ranges of break-up and the type of break-up.

4 Phase-field Models

The models used for the study of elastic stress induced instabilities can be very broadly classified as atomistic models and continuum models. The Discrete Atom Method (DAM) is an example of the atomistic method. On the other hand, the continuum models can further be broadly classified as sharp interface and diffuse interface models. Most of the theoretical studies described in the previous section, for example, are sharp interface models. There are numerical implementations (at times based on the finite element method) of these sharp interface models (see for example,[216]). However, for the study of microstructural instabilities, as we show below, the diffuse interface models are the most ideal.

In the diffuse interface models, the microstructure is described using field variables (that is, variables which are defined for all space points at all times) and their derivatives. These field variables are also called order parameters. The order parameters typically take a constant value in the bulk phases and change from one bulk value to another in the interface region. Thus, the interface is defined as the region over which the order parameter changes. Hence, these models are called diffuse interface models. In these models, the bulk phases are defined by the constant value that the field variable takes inside of them. Hence, these models are also called phase field models—to indicate that different phases are denoted by the field variables taking specific values.

There are several different ways in which one can understand phase field models. Here we list a few of these viewpoints—though, these viewpoints are not exclusive.

Phase field models can be thought of as a mathematical strategy to find solutions for hard-to-solve sharp interface models.[217–219] In such a scenario, we artificially assume a width to an interface, which, in reality, a plane of zero width. Such artificial, diffuse interface allows us to solve the resultant partial differential equations fairly easily. In such a viewpoint, the attempt is always to show that in the limit of the interface width going to zero, we obtain the corresponding sharp interface models, and hence, in the limit of the interface width going to zero, we obtain the solution to the sharp interface problem from the corresponding diffuse interface solution. This viewpoint can be considered as a purely mathematical viewpoint because many physical interfaces are indeed diffuse.

Phase field models can also be thought of as partial differential equations that lead to interesting patterns as solutions. In this viewpoint, which is also relatively mathematical, the emphasis is on the solutions obtained. A classic example of this viewpoint is the attempt of Alan Turing[220] to look at pattern formation (what he called as chemical morphogenesis) as a reaction-diffusion equation.

Another prominent viewpoint is to think of phase field models as continuum models (derived from statistical physics) that lead to interesting patterns as solutions.[221,222] As in the case of biological pattern formation models, in this viewpoint also, the emphasis is on the solutions obtained. However, here an attempt is also made to connect the patterns obtained to the underlying physical processes and statistical mechanics. To that extent, this viewpoint is more physics based.

The viewpoint (which we will take in this review, and which we call as the materials science based approach) is to consider phase field models as non-classical diffusion equations. In this viewpoint, we begin by modifying the classical thermodynamics of materials. In classical thermodynamics, the interface width is arbitrarily assumed (typically, zero—though not always); and, in calculations (such as in phase diagram construction) the interface contribution is further assumed to be negligible. If we incorporate this interface contribution and allow the system to choose the interface width consistent with the imposed thermodynamic variables and constraints, the resultant non-classical thermodynamics (along with certain constitutive laws), as we show below, leads to equations which are non-linear diffusion equations. This was the approach pioneered by Cahn and Hilliard in formulating the Cahn-Hilliard equation[223] and explained very lucidly in his pedagogical article by Hilliard.[169]

The contribution of Cahn and Hilliard (based on the earlier atomistic studies of Hillert) is to show that this wavelength limit is set by interfacial energy of the incipient interfaces in the system and to get this limit out of the model, the interfacial energy contribution should be incorporated into the free energy. In the next subsection, we will indicate the modification to the free energy and the derivation of the Cahn-Hilliard equation. This is one of the two canonical phase field equations. In the following subsection, we will indicate the other canonical phase field equation called Allen-Cahn equation (or, sometimes Time Dependent Ginzburg-Landau (TDGL) equation, or, simply, Ginzburg-Landau equation). All phase field models can be thought of as a combination of these two models. These two subsections will also set the stage for us to describe the process of formulating phase field models in a more abstract fashion.

4.1 Cahn-Hilliard equation
The classical Gibbs free energy in a binary alloy is a function of composition. The derivative of this free energy with respect to the A or B atoms gives the corresponding chemical potential. Using the chemical potential in the modified Fick's first law in combination with law of conservation of mass leads to the classical diffusion equation.

Cahn and Hilliard showed that in order to account for interfacial energy contribution to the free energy, the free energy should be made a function of not just composition but also its derivatives (spatial, such as gradient, curvature, aberration and so on). This implies that the free energy is not a function but functional. Specifically, in the case of a binary alloy (assuming isotropy or cubic anisotropy), Cahn and Hilliard showed that the free energy functional is of the form

$$G(c, \nabla c, ...) = N_V \int_V dV[f_0(c) + K \, |\nabla c|^2] \qquad (73)$$

where K is the gradient energy coefficient (assumed constant), and $f_0(c)$ is the bulk free energy density.

Since the free energy is a functional, the chemical potential is given by the variational derivative of the free energy functional (the Euler-Lagrange equation):

$$\mu = \frac{\delta(G/N_V)}{\delta c} = \frac{\partial f_0}{\partial c} - K\nabla^2 c \qquad (74)$$

Using this chemical potential, we can define the flux as

$$\mathbf{J} = -M\nabla\left[\frac{\partial f_0}{\partial c} - K\nabla^2 c\right] \quad (75)$$

This flux, along with the conservation of mass, leads to

$$\frac{\partial c}{\partial t} = \nabla M\nabla\left[\frac{\partial f_0}{\partial c} - K\nabla^2 c\right] \quad (76)$$

Thus, the Cahn-Hilliard equation is given as

$$\frac{\partial c}{\partial t} = M\frac{\partial f_0}{\partial c}\nabla^2 c - MK\nabla^4 c \quad (77)$$

where we have assumed the mobility to be a constant.

Comparing this equation with the classical diffusion equation, we see that there is an extra non-linear term ($\nabla^4 c$).

4.2 Allen-Cahn equation

The Allen-Cahn equation can be derived in a very similar fashion. Let us assume that the microstructure is described using an order parameter ϕ. For simplicity, we assume that the ϕ parameter takes to distinct values (say, zero and unity) in two phases and takes values between zero and unity in the interface region. Let $f_0(\phi)$ be a double-well potential with minima at zero and unity. Let us consider a free energy functional that describes the thermodynamics of the system:

$$G(\phi, \nabla\phi, ...) = N_V \int_V dV[f_0(\phi) + K|\nabla\phi|^2], \quad (78)$$

where K is the gradient energy coefficient (assumed constant).

In this case also, we can define a chemical potential:

$$\mu = \frac{\delta(G/N_V)}{\delta\phi} = \frac{\partial f_0}{\partial\phi} - K\nabla^2\phi. \quad (79)$$

In the Allen-Cahn case, we assume that the order parameter is not a conserved quantity (unlike the case of composition where $\frac{d}{dt}[\int c dV] = 0$). Hence, we assume the following constitutive law for the rate of change of order parameter:

$$\frac{\partial\phi}{\partial t} = -L\mu \quad (80)$$

where L is the relaxation parameter.[224]

Hence, one obtains the Allen-Cahn equation as

$$\frac{\partial\phi}{\partial t} = LK\nabla^2\phi - L\frac{\partial f_0}{\partial\phi}. \quad (81)$$

This equation is also known as TDGL equation or reaction-diffusion equation, since it is very similar to diffusion equation except for the non-linear polynomial is ϕ, which is like a source/sink term due to chemical reactions.

4.3 Incorporating elastic stress effects

Since we concentrate on the elastic stress induced microstructural instabilities in this review, the incorporation of elastic stress effects into the formulation is a key step. The incorporation of elastic stress effects into the phase field models is achieved by adding the elastic energy $F^{el} = \frac{1}{2}\int\sigma^{el}\varepsilon^{el}$ to the free energy functional. The elastic stress and strain fields are obtained by solving the equation of mechanical equilibrium.

In all these models, since the time scales of elastic relaxation are much larger than the diffusional time scales, the phase field equations and the equation of mechanical equilibrium are solved sequentially, assuming that for any given order parameter field, the elastic fields equilibrate instantaneously; in addition, the eigenstrain or the elastic moduli or both are slaved to the order parameter. The resultant equation of mechanical equilibrium is solved with either imposed strain or applied traction boundary conditions.

In models of microstructure evolution, it is very common to assume that the domain of computation is a representative volume element; in other words, it is common to use periodic boundary conditions.

As discussed earlier, in most cases of interest, the elastic moduli are anisotropic (at least cubic) and inhomogeneous; there are eigenstrains (primarily, due to coherency) and applied stresses. Hence, slaving the eigenstrains and elastic moduli to the order parameters makes solving the equation of mechanical equilibrium becomes one of homogenisation problem.

The equation of mechanical equilibrium in coherent, anisotropic and inhomogeneous systems can, of course, be solved using finite element techniques; there are several studies that use finite element techniques. However, in phase field models, in certain cases, like, for example, in the case of spinodal decomposition, such finite element techniques can become very difficult from an implementation/computational cost point of

view, since to capture interface very fine meshing is needed and the microstructure is full of interfaces. In addition, as the microstructure evolves, the mesh also needs frequent updating. Hence, Fourier transform based spectral techniques are very widely used and are quite successful.

4.4 Formulation

As noted at the beginning of this article, microstructure is nothing but the size, shape and distribution of interfaces; specifically, when we are studying elastic stress driven microstructural instabilities, we are interested in the formation, disappearance, break-up and/or merger of interfaces in elastically stressed systems. Thus, any model that we formulate to study stress driven microstructural instabilities should be capable of describing the microstructure (geometry or topology), its energetics (thermodynamics), and kinetics; in addition, since we are interested in stress driven microstructural changes, our energetics should include the strain energy, which, in turn, should be calculated using the appropriate physics.

The two canonical phase field models that we discussed above, namely the Cahn-Hilliard equation for systems with conserved order parameters, and Allen-Cahn equations for systems with non-conserved order parameters lead to non-linear diffusion equations (from a mathematical point of view; note that physically, while Cahn-Hilliard is actually a modified diffusion equation, Allen-Cahn is not). However, from the derivation of these two equations it is clear that the general formulation of phase field models (which are nothing but a combination of these two types of equations) consists of the following steps:

* **Description of microstructure (the geometry/topology)**
  The first step in formulating a phase field model is to identify the order parameter that describes the microstructure. The order parameter can be a conserved quantity (such as composition) or a non-conserved quantity (such as ordered domain of a given type).
* **Thermodynamics**
  The second step is to describe the thermodynamics of the system. We do this by defining the free energy or entropy functional; these thermodynamic functionals are given in terms of the order parameters and their spatial derivatives. In our viewpoint, it is such thermodynamic description (in terms of functionals) that make phase field models what they are. If the thermodynamics is

described using classical free energy functions (without (at the least) the gradient terms), the resultant partial differential equations will lead to sharp interface and not diffuse-interface description.
* **Kinetics**
  Given a free energy functional, one can define the chemical potential. In terms of the chemical potential, then, there are two constitutive laws that we use, which introduce the kinetics—how fast or slow the system relaxes to its equilibrium (since, for equilibrium, the Euler-Lagrange equations should equal zero): in the case of Cahn-Hilliard equation, it is the mobility and in the case of Allen-Cahn equation, it is the relaxation parameter.
* **Conservation laws and other physics**
  As in the case of Cahn-Hilliard equation, after the introduction of kinetics, we may have to impose any other relevant conservation laws such as conservation of mass, energy and charge. In addition, in the case of elastically stressed systems that we discuss in this paper, the free energy will also consist of the elastic energy terms. These elastic energy terms are to be computed using the relevant physics: that is, the equation of mechanical equilibrium should be solved under appropriate boundary conditions and the resultant stress and strain fields along with applied stresses (if any) should be used to compute the elastic energy term. Similar process has to be carried out if the free energy contains electric, magnetic or any such other energy terms that are relevant.[225]

At this point, it is to be emphasised that phase field modelling is a methodology; for example, for the same problem, there could be more than one description in terms of order parameters and the energetics; this depends on the level of detail that we wish to incorporate. There is no "the" phase field model for any given problem. A good example of this, in our context, is to think of phase field models for elastically stressed systems: one can consider scalar order parameters and make the eigenstrains slaves of such order parameters (which is the more common approach); however, one can also think of the strains as the order parameters and evolve them by writing corresponding free energies (if we can). Similarly, in the case of Ni-base superalloys, for example, if Anti-Phase Boundary (APB) related physics is not important, they can be modelled using a single composition order parameter. However, if APBs are important, in addition, one should introduce three additional

non-conserved order parameters so that the four variants can be completely described.

From the description above, yet another viewpoint on phase field models emerges. In this viewpoint, phase field models are partial differential equations that describe the evolution of order parameters that describe microstructures; the order parameters are field variables; they take constant values in the bulk and change in the interface region and thus, highlight the interfaces and hence help us understand the formation of microstructures and their evolution.

There are two characteristics of the solutions of the phase field equations that are very important. The first is of course the diffuse interface solution (which is a direct consequence of the inclusion of gradient terms); this means that there are no discontinuities in the domain and hence there is no need for tracking of interfaces (to impose jump conditions for example). This makes the numerical solutions much easier and also makes the processes of dealing with formation, disappearance, merger and splitting of interfaces fairly easy. The second is that the interface physics (that which is relatable to the interfacial energy primarily and not so much interface structure—such as Gibbs-Thomson effect, for example) are automatically taken into account in these models. There is no need to incorporate them separately as is sometimes done in sharp interface models.

4.5 Parameters, non-dimensionalisation and numerical implementations

The parameters that enter the phase field model for stress induced microstructural evolution are the following:

- **Related to the thermodynamics of the system**
  Bulk free energy density and the gradient energy coefficients;
- **Related to the kinetics**
  The mobilities and relaxation parameters; and,
- **Related to equation of mechanical equilibrium**
  The eigenstrains and the elastic moduli along with their dependence on the order parameters; and applied stresses or imposed strains.

In addition, there are numerical implementation related parameters that enter the calculations such as the domain size, the spatial grid size, and the time-steps of integration. Finally, in the numerical solution of the equation of mechanical equilibrium, there are magic numbers that enter the calculation such as convergence criterion for elastic fields.

In general, while solving equations on a computer, it is preferable that the equations are non-dimensionalised. This makes the computations robust and can help avoid repetitions in calculations. A careful choice of non-dimensionalisation is also essential to carry out meaningful simulations. Let us consider a typical microstructure in which the interface is a few lattice parameters wide, say 1 nm or so. To capture the interface in the numerical model, we need nearly six to eight mesh points. Assuming that the interface will be captured using eight mesh points, one can see that the spatial discretization corresponds to about 1.25 Å. This can, at times, be very restrictive. Appropriate non-dimensionalisation can help overcome this problem as explained below.

In the classical Cahn-Hilliard model, there are two interfacial parameters, namely, the width and energy. One can use the parameters associated with the thermodynamics, namely, the energy barrier between the two phases in the bulk free energy density and the gradient energy coefficient by non-dimensionalising these quantities using the interfacial energy and interfacial width, while the kinetic parameters are used to non-dimensionalise time. Such non-dimensionalisation helps us study bigger systems and is described in detail in.[161]

At this point, it is also clear that there are several quantities that enter the phase field models, which are difficult to measure experimentally. For example, the coherency strains, the moduli and their dependence on composition, the interfacial energy, and the mobility are difficult to measure experimentally, though, reliable measurements of the bulk free energies (in the form of CALPHAD data, for example) are available; in some cases, diffusivity is also available.

In Cahn and Hilliard's work, in addition to connecting their bulk free energy density term to a regular solution model, they also attempted to relate the gradient energy coefficient to the bond energies. However, these attempts are not very successful. Hence, in most phase field models, at present, it is far more easier (and reliable) to get trends than to get actual quantitative information though attempts are being made to make the phase field models more quantitative; see for one of the early attempts.[226]

Finally, the phase field equations can be solved using any of the available numerical techniques: finite difference, finite volume, finite element (see for example[227,228] and references therein), boundary integral method[19] and spectral techniques.[229]

As noted by,[228] though using finite element method for Allen-Cahn equations is easy, for Cahn-Hilliard method higher order interpolation methods are needed. Simulating local mass flux and handling topological singularities are very difficult in boundary integral methods; the method might also require preconditioners to solve the resulting system of equations.[19]

Khachaturyan, Chen and their co-workers pioneered the use of spectral techniques. Spectral techniques have several advantages: they automatically incorporate periodic boundary conditions that are the relevant boundary conditions for the representative volume elements. Even though they do not convert the partial differential equation into an ordinary differential equation since phase field models consist of non-linear terms, they still can be implemented using semi-implicit techniques and hence allow for relatively larger time steps and also result in spectral accuracy. They can handle higher order derivatives very well. One disadvantage of spectral techniques, of course, is that boundary conditions other than periodic boundary condition is difficult to incorporate, which can be done fairly easily in finite difference techniques for example.

In terms of numerical implementation, even though finite difference techniques are more involved, they can be easily parallelised unlike spectral techniques. However, in recent times, the GPU based parallelisation of FFT (such as CUDAFFT) has given some advantage in terms of parallelization to spectral techniques.

4.6 Benchmarking against analytical solutions

Several authors have carried out more formal asymptotic analysis for phase field models incorporating elastic stress effects; see Fried and Gurtin,[149] Leo et al.[27] and Garcke and Kwak[230] for some representative examples.

When it comes to numerical implementation of phase field models, benchmarking the numerical solutions obtained from phase field models against classic elastic solutions (in those cases where they are available) is very important. Such benchmarking serves to show that the numerical implementation is correct. In addition, though not as rigorous as the analysis of, for example, Garcke and Kwak, such benchmarking can be thought of as an engineering approach to checking on the correctness of phase field formulation. In this subsection, we list examples of such benchmarking from some of our work; similar benchmarks have been reported by other authors too.

- Chirranjeevi et al.[231] have confirmed that the phase field models do indeed show the symmetric and anti-symmetric break-up of films as predicated by Sridhar et al.[202] Further, at the very early stages of the break-up, the maximally growing wavelength compares well with the analytical solution.[161]

- Gururajan and Abinandanan[168] have obtained all the five regions identified by Schmidt and Gross.[184] In addition, they have also verified that the results from the phase field model compare well with Eshelby solution for inclusions and inhomogeneities (including voids),[7] and the homogeneous strain[8] for homogeneous alloys.[161]

- Mukherjee et al.[232] show that phase field models predict the curvature and coherency driven Gibbs-Thomson effect very well; further, in 1-D, in systems with no coherency strains, the growth rates are shown to agree well with the classical solutions of Frank[233] and Zener.[234]

4.7 Spinodal phase separation: Suppression and promotion

The phase field implementation of phase separation in elastically stressed systems have been many: see for example.[166,167,235–242] As noted above, the presence of elastic stresses or strains tends to suppress spinodal. However, when the system does undergo spinodal, the composition modulations in elastically softer directions grow leading the phase separation that is anisotropic.

If the system is elastically inhomogeneous, the harder phase becomes more compact but deviates from spherical shape and takes shapes that are consistent with their elastic anisotropy; for example, in cubic systems they become cuboids; they also preferentially align along the elastically soft directions. In addition, the coarsening rates in such systems after phase separation is slow. Finally, as we show below, the compact precipitate phases might split; and, in the presence of applied stresses, they coarsen preferentially along certain directions.

However, if there are imposed strains on the system (for example, as in the case of an epitaxially grown thin film undergoing spinodal decomposition), then the elastic stresses can promote spinodal decomposition even outside the chemical spinodal.[51] In this section, using the analytical solution derived in the previous section, we extend the analysis of Cahn and show that the coherent spinodal region extends beyond chemical spinodal.

3.7.1 Computing the spinodal: Here we assume a regular solution model for computing

the spinodal lines. According to Cahn,[170] the chemical spinodal is given by,

$$\frac{\partial^2 G}{\partial c^2} = 0, \tag{82}$$

where,

$$G = G_A(1-c) + G_B c + RT[c \ln c + (1-c)\ln(1-c)]$$
$$+ \ \Omega c(1-c), \tag{83}$$

where G is the molar Gibbs free energy, R is the Universal Gas constant and Ω is the molar heat of mixing. The critical temperature is given by:

$$T_c = \frac{\Omega}{2R}. \tag{84}$$

For the coherent spinodal in the plane stress setting assuming isotropic elasticity, we have:

$$\frac{\partial^2 G}{\partial c^2} + Y\eta^2 V = 0, \tag{85}$$

where the Young's modulus Y is a function of homogeneous alloy composition and V is the molar volume of the homogeneous alloy under question.

Now we consider the situation where the elastic modulus of the system is composition dependent and the system is subjected to an applied homogeneous strain (constrained spinodal). We start out with a homogeneous alloy having a composition c_0, whose strain energy density is given by:

$$W_E^0 = \frac{1}{2}[Y_A + (Y_B - Y_A)c_0]e^2, \tag{86}$$

where we assume the lattice of an undecomposed 50:50 alloy to be the reference. In the presence of a composition modulation, the strain energy density becomes:

$$W_E^1 = \frac{1}{2}[Y_A + (Y_B - Y_A)c][e - \eta(c - c_0)]^2$$

Now, assuming $c - c_0 = A\cos\beta x$, we get the expression of the total strain energy as:

$$W = \int_\Omega [W_E^1 - W_E^0]d\Omega$$
$$= \frac{1}{2}\int_\Omega [Y_A\eta^2 + 3\eta^2(Y_B - Y_A)c_0$$
$$- 2\eta e(Y_B - Y_A)](c - c_0)^2 d\Omega. \tag{87}$$

This defines the *constrained spinodal* as:

$$\frac{\partial^2 G}{\partial c^2} + [Y_A\eta^2 + 3\eta^2(Y_B - Y_A)c_0 - 2\eta e$$
$$\times (Y_B - Y_A)]V = 0 \tag{88}$$

where V denotes the molar volume.

In Fig. 5, we show the chemical, coherent and the constrained spinodal lines. The asymmetry in the spinodal lines is a characteristic of the composition dependent modulus. The spinodal lines were constructed using the following values for the different parameters (the strains are measured with respect to a 50:50 alloy): $\Omega =$ 10000 $J/mol - K$, $Y_A = 312.5\ GPa$, $Y_B = 625\ GPa$, $\eta = 0.02$, $v = 0.3$ and $V_A = V_B = 10^{-5}$ m³/mol. For obtaining the different constrained spinodals, we applied different homogeneous strains: $e = 0.04$ leads to the constrained spinodal extending beyond the chemical spinodal; $e = 0.01$ leads to the constrained spinodal lying between the coherent and the chemical spinodal; $e = -0.02$ leads to the constrained spinodal being restricted inside the coherent spinodal. Thus, our choice clearly demonstrates the different possibilities for the constrained spinodal in an epitaxial systems where large tensile and compressive imposed strains are possible.

4.8 *Particle splitting*

Wang et al.[236] used phase field modelling to show particle splitting that was achieved by the nucleation of matrix phase at the centre of the precipitate.
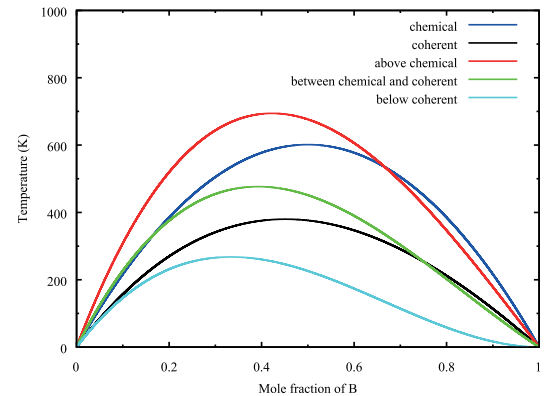
Figure 5: Chemical, coherent and the constrained spinodal lines. Notice that for different values of applied homogeneous strain, the constrained spinodal can be made to lie within the coherent spinodal, or outside of coherent spinodal but within the chemical spinodal, or, even outside the chemical spinodal.

However, in this model, the elastic moduli of both the phases is assumed to be the same and the elastic energy per unit volume was varied. This is not very realistic. On the other hand, Wang and Khachaturyan,[165] using the same homogeneous moduli approximation, showed that high elastic anisotropy leads to cuboidal precipitates, which, due to the presence of corners that promote "earing" (due to the point effect of diffusion), can lead to star shaped precipitates; however, the stars never split (though, initial star shaped particles studied using sharp interface models (level set method) showed morphologies closer to split morphologies: see for example, Zhao et al.[243]—albeit assuming inhomogeneous elasticity.

Luo et al.[244] reported particle splitting like morphologies as due to nucleation of ordered precipitates at dislocations (assuming homogeneous moduli approximation). Similarly, the phase field study of Banerjee et al.[245] showed that it is possible to obtain experimentally seen splitting morphologies through particle coalescence (as also experimentally shown by[73–75]).

There are other phase field models that report splitting (in elastically inhomogeneous systems). Li and Chen[166] report particle splitting in systems with applied stresses. Boussinot et al.[246] attribute particle splitting to elongated particles in an unfavourable direction under applied stress. Similar conclusions were also drawn by Lee[247] using DAM method and Leo et al.[248] using a sharp interface model; our own work on particle splitting using phase field modelling also supports this conclusion.[161]

Cha et al.[249] and Kim et al.[250] report splitting as due to elastic anisotropy and diffusion induced instability (which, in some sense, is closer to ATG instability since they also assume elastic inhomogeneity); The elastic anisotropy leads to cuboidal precipitates; the corners lead to earing of the precipitates as they grow; this earing enhances the elastic stress fields (like in ATG instability) and hence leads to splitting.

Zhu et al.[240] argue that splitting during coarsening is due to the geometric aspect of high aspect ratios of length to width of the particles.

Leo et al.[248] have used sharp interface model to show that deviatoric applied stresses and non-dilational misfit strains (in the absence of applied stresses) can lead to particle splitting. Unfortunately, as far as we know, there are no phase field models that report splitting in systems with non-dilatational misfit or deviatoric applied strains. This would be an interesting problem that can be solved with existing implementations of phase field models.

Further, Lee[251] classifies elastic splitting instability into two types, namely, commensurate and incommensurate; incommensurate instability is the instability due to the elastic anisotropy of the matrix and precipitate phases being of opposite signs. Lee simulated both types of splitting using Discrete Atom Method and indicated that splitting can happen even in elastically isotropic systems.[247,252–254] There are no detailed studies on incommensurate splitting instability using phase field models—though, this is again a problem that can be easily studied using available phase field models.

To summarise, currently, there are at least two valid mechanisms by which 'split'-like patterns can be formed. In inhomogeneous systems, it is the interactions of anisotropy induced geometries interacting with diffusion fields leading to stress fields that result in actual splitting (through an ATG like mechanism). The second one is the coalescence of different ordered domains coming together during coarsening. Note that while the first mechanism necessarily involves elastic inhomogeneities, the second can operate even in homogeneous systems (and while the first one is a true elastic stress induced instability, the second one is not). Finally, the applied stress fields, non-dilatational eigenstrains and differences in elastic anisotropy between the matrix and precipitate phases can also have a strong say on splitting—though they are not explored experimentally enough (nor by modelling in an exhaustive manner) at the moment.

Our foregoing discussion is also very instructive at another level. It clearly shows that several different mechanisms can lead to the same microstructural feature. It also shows that phase field models (or any modelling study for that matter) can not only be used to verify a proposed mechanism, but also for advancing new mechanisms that can then be checked through experiments. Thus, while 'equations without a phenomenological background remain a formal game',[255] these games can be very fruitful if they lead to such experimental validations and verifications. However, such verifications also imply that the parameters used in simulations are realistic; checking that indeed all the parameters used in the simulations are realistic becomes difficult due to the different non-dimensionalisations used. Hence, indicating to the readers the translation of simulation parameters in terms of what they correspond to in real life (which, unfortunately, is not the current practice) will make the simulation studies more grounded in phenomenology.

4.9. *Rafting*

There have been several papers questioning elastic energy based explanations of rafting. For example, one of the conclusions of Ichitsubo et al.[256] reads as follows:

> In the coherent elastic regime, the rafted structure cannot be realized unless the elastic misfit exists, and both signs of lattice misfit and external stress are not relevant to the choice of the rafted structures; the only 0 0 1 rafted structure can be formed in any conditions. This indicates that the actual rafting phenomenon cannot be explained within the elastic regime.

There are also claims that plastic prestrain is essential for rafting. For example, Tinga et al.[257] write:

> Whereas a certain amount of plastic deformation is a requirement for the onset of rafting, the presence of an external stress surprisingly appears not to be a requirement to sustaining the rafting process.

Finally, there are studied based on elastic energy calculations that the raft structure itself is elastically unstable[258] and phase field models to simulate the collapse of the rafted structure.[259]

The most important contribution from phase field modelling is to show that purely elastic stress driven rafting is possible. There have been a series of phase field studies showing purely elastic stress driven rafting: Li and Chen,[260,261] Leo et al.,[248] Zhu et al.,[240] Gururajan and Abinandanan[168]

and Boussinot et al.[246] In Fig. 6, and 7, we show examples of purely elastic stress driven rafting;[161] these figures vouch for the correctness of the predictions of Schmidt and Gross.[184]

Of the elastic stress driven rafting studies, Boussinot et al.[246] is the most complete; it not only includes the compositional order parameter but also the non-conserved order parameters to account for the different variants of the precipitate phase. These studies show the correctness of the thermodynamic models based on Hookean elasticity.

As in the case of incommensurate splitting shown by Lee,[251] incommensurate rafting is also possible.[184] However, a detailed study of rafting due to such differences in anisotropy and Poisson's ratio (which is well within the capabilities of the current formulations and implementations) has not yet been made.

The second important contribution of the phase field models is to indicate the kinetic paths of rafting.
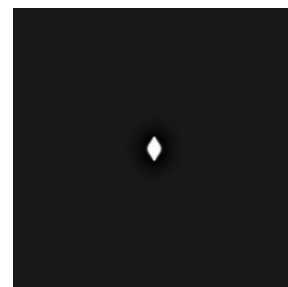
Figure 6: Figure from:[161] A very soft precipitate ($\delta = 0.01$) under compressive stress ($\sigma^A = -0.01\,G^m$ along *x*-axis) in an elastically isotropic system after 300 time units; numerical simulation corresponding to Region 5 of the Figure 2.

(a)　　　　　　　　(b)
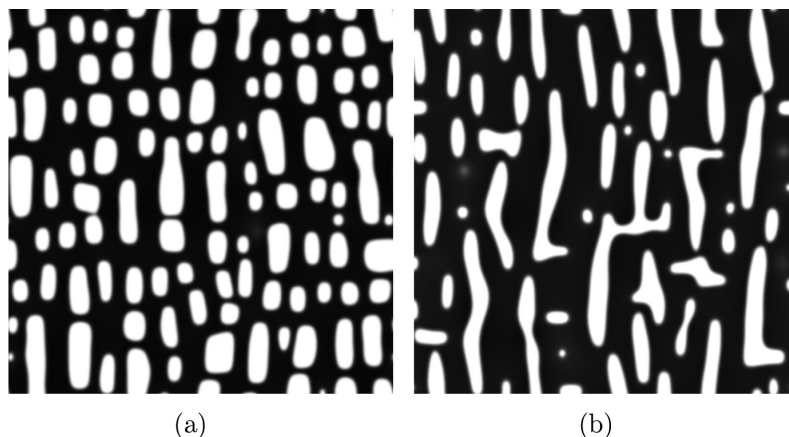
Figure 7: Figures from.[161] Rafting in an anisotropic system (Zener anisotropy parameter: $A_z = 3$) of (a) hard particles ($\delta = 2$) under a tensile stress, and, (b) soft particles ($\delta = 0.5$) under a compressive stress; stresses are applied along the *y*-axis and, the magnitude of the stress is 1% of the shear modulus of the matrix. microstructures after 3000 time units.
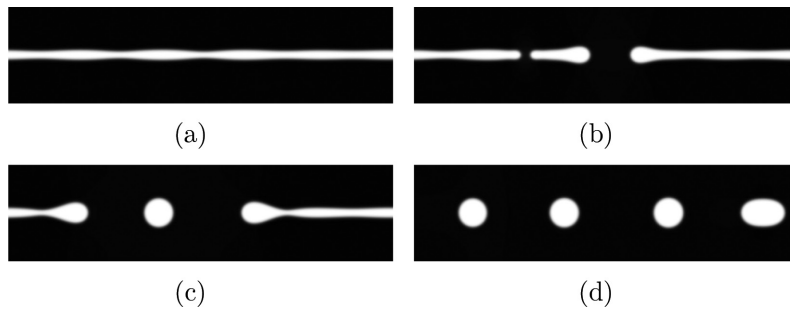
Figure 8: Figures from.[161] Symmetric break-up and late stage evolution in a thin film assembly in an elastically isotropic, inhomogeneous ($\delta = 2$) system: morphology at (a) 115000, (b) 122000, (c) 129000, and (d) 143000 time units. $L_x = 512$; $L_y = 128$; $h = 10$.

In this regard, the pure elasticity based phase field models described above have limited use. However, since in the practical scenario, there is always plastic activity, and since plastic activity can give rise to very different kinetics and kinetic paths, it becomes important to incorporate plasticity in the phase field models; there have been a few such improved phase field models in the last few years.[262,263]

4.10 ATG instabilities

Kassner and Misbah[264] and Kassner et al.[265,266] studied ATG instabilities by modelling a stressed solid in contact with its melt. Kassner et al.[265] show that the reference state to measure displacements (and hence strain and stress) is important and different choices lead to different evolution equations; they also show that the model, in the sharp interface limit, recovers the continuum equations for ATG instabilities. Further, Kassner et al. also show that phase field models themselves can be used to build more complex sharp interface models.

Phase field models of ATG instabilities in the case of films in contact with vapour or vacuum is more common; see for example.[267–274] In addition, there are also phase field models that study ATG in the dynamic setting of growing films; see for example.[275–280] In addition to surface diffusion being a relatively faster process, an important physics associated with these problems is the interfacial anisotropy and some of these models do incorporate interfacial energy anisotropy.[268,276] Since typical analytical studies of ATG instabilities assume isotropic interfacial energies,[202] phase field studies are helpful to relax this assumption and see the effect of the same.

Phase field models of ATG instabilities in the cases of film assemblies are studied by Chirranjeevi et al.[231] and Zaeem and Mesarovic.[281] As noted in the previous section, in the case of solid-solid ATG instabilities, there are more than one mode of break-up, namely, symmetric and anti-
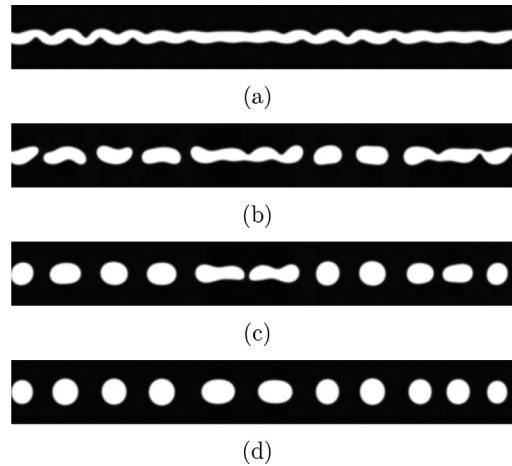
Figure 9: Figures from.[161] Anti-symmetric break-up and late stage evolution in a thin film assembly in an elastically isotropic, inhomogeneous ($\delta = 4$) system: morphology at (a) 20000, (b) 25000, (c) 28000, and (d) 34000 time units. $L_x = 1024$; $L_y = 128$; $h = 20$.

symmetric are possible. Phase field models are able to capture these different modes of break-up under appropriate conditions. Further, using the phase field models, it is also possible to study long-time dynamics (which could be, and indeed is, very different from early stage dynamics—see Figs. 8 and 9). Finally, it is known that the effect of interaction between the different layers is important[282,283] and phase field models are capable of dealing with them as well as the effect of elastic anisotropies.[231]

Zaeem and Mesarovic[281] extend the study further and look at the effect of metastable intermediate phase. In addition, they show that there is homogenisation for very thin layers. However, as we have seen in the spinodal section, in such films, the homogenised region could be a phase separated region albeit with a morphology different from thin films. This problem has not

yet been explored in detail even though it is well within the capabilities of current models and implementations.

5 Conclusions

In this review, using stress effects on spinodal phase separation, particle splitting, rafting and ATG instabilities, we have shown that phase field models are quite successful in the study of elastic stress induced microstructural instabilities. In some cases, such as rafting, they have acted as computer experiments to access regimes that are experimentally well near impossible to access. In some cases, such as particle splitting, phase field models have shown that there could be more than one mechanism leading to the observed microstructural features. In the case of ATG instabilities and spinodal phase separation, they are very helpful to understand some of the experimental observations; this understanding can be translated into better control of phenomenon. We have also identified some problems that can be tackled with the current phase field formulations and numerical implementations but have not yet been studied in detail.

From the review, it is clear that there has to be more attempts to connect phase field parameters either with phenomenological data or with data from other methods (such as first principles and atomistic simulations) in order to make phase field studies more quantitative. We found very few papers tackling such problems. There are also relatively lesser number of studies on 3-D systems. We believe that the GPU based computing will change that and expect more 3-D studies in the next few years.

We also came across several attempts towards extending the models to incorporate interfacial energy anisotropy and different aspects of plasticity; see for example the study on stressed incoherent solid-solid interfaces by Paret,[284] effect of coupling of defects such as dislocations, coherent interfaces, vacancy and interstitial discs on microstructural evolution,[285] spinodal phase separation induced by irradiation in the presence of dislocations,[286] phase separation coupled with large elastic and large elastic-plastic deformations during Lithiation in Li-ion battery electrodes,[287,288] phase field modelling misfit accommodation by considering a precipitate growing into a finite elastic-perfectly plastic matrix,[289] and, phase field model to study the stability of ordered array of islands by considering the elastic interaction between them.[290] In the near future, we expect that there will be more studies incorporating interfacial anisotropies and plasticity.

There are also attempts to study strain gradient theories of Eshelby problem formulation;[291] we believe that phase field formulation of such problems will be very interesting. There are a few attempts in this direction: see for example, the strain gradient models (to introduce characteristic length scales of microstructure to study mechanical behaviour) based phase field modelling to study strongly elastoviscoplastic systems.[292] Finally, the studies that include other physics such as electric and magnetic fields along with elasticity will also become more important as is clear from several recent attempts to study electrochemical processes such as corrosion and studies such as the phase field model for morphological evolution of vesicles in electric fields.[293]

To conclude, even though the study of elastic stress effects on material behaviour started by Gibbs about 140 years ago, their study using phase field models is still open; and, the open problems span the entire range—from theoretical formulations, to numerical implementations to materials science concepts—not to mention experimental verifications and validation.

References
1. G.J. Schmitz. Microstructure modeling in Integrated Computational Materials Engineering (ICME) settings: Can HDF5 provide the basis for an emerging standard for describing microstructures? *JOM* **68**, 77–83 (2016).
2. J.W. Martin, R.D. Doherty and B. Cantor, *Stability of microstructure in metallic systems*, Cambridge University Press, Cambridge, UK, second edition (1997).

3. P. Fratzl, O. Penrose and J.L. Lebowitz, Modeling of phase separation in alloys with coherent elastic misfit, *Journal of Statistical Physics* **95**, 1429–1503 (1999).

4. M. Doi, Elasticity effects on the microstructure of alloys containing coherent precipitates, *Progress in Materials Science* **40**, 79–180 (1996).

5. W.C. Johnson, Influence of elastic stress on phase transformations, In H I Aaronson, editor, *Lectures on the theory of phase transformations,* Chapter 2, pages 35–134, TMS, Pennsylvania, USA, second edition (1999).

6. P.W. Voorhees and W.C. Johnson, The thermodynamics of elastically stressed cyrstals, *Solid State Physics* **59**, 1–201 (2004).

7. T. Mura, *Micromechanics of defects in solids.* Kluwer Academic Publishers, London, UK, second edition (1987).

8. A.G. Khachaturyan, *Theory of structural transformations in solids*, John Wiley & Sons, Inc., New York, USA (1983).

9. L.-Q. Chen, Phase-field models for microstructure evolution, *Annual Review of Materials Research* **32**(1), 113–140 (2002).

10. W.J. Boettinger, J.A. Warren, C. Beckermann, and A. Karma, Phase-field simulation of solidification, *Annual Review of Materials Research* **32**(1), 163–194 (2002).

11. I. Steinbach, Phase-field models in materials science. *Modelling and Simulation in Materials Science and Engineering* **17**, 073001 (31pp) (2009).

12. K. Thornton, J. Agren and P.W. Voorhees, Modelling the evolution of phase boundaries in solids at the meso- and nano-scales, *Acta Materialia* **51**(19), 5675–5710 (2003).

13. N. Moelans, B. Blanpain and P. Wollants, An introduction to phase-field modeling of microstructure evolution, *Computer Coupling of Phase Diagrams and Thermochemistry* **32**, 268–294 (2008).

14. Y. Wang and J. Li, Overview no. 150, Phase field modeling of defects and deformation, *Acta Materialia* **58**, 1212–1235 (2010).

15. H. Emmerich, Advances of and by phase-field modelling in condensed matter physics, *Advances in Physics* **57**, 1–87 (2008).

16. R. Phillips, Multiscale modeling in the mechanics of materials. *Current Opinion in Solid State and Materials Science* **3**, 526–532 (1998).

17. M, Militzer, Phase field modeling of microstructure evolution in steels, *Current Opinion in Solid State and Materials Science* **15**, 106–115 (2011).

18. M.F. Henry, Y.S. Yoo, D.Y. Yoon and J. Choi, The dendritic growth of γ' precipitates and grain boundary serrtion in a model nickel-base superalloy, *Metallurgical Transactions A* **24A**, 1733–1743 (1993).

19. H.-J. Jou, P.H. Leo and J.S. Lowengrub, Microstructural evolution in inhomogeneous elastic media, *Journal of Computational Physics* **131**, 109–148 (1997).

20. Y.S. Yoo, Morphological instability of spherical γ' precipitates in a nickel base superalloy, *Scripta Materialia*, **53**, 81–85 (2005).

21. B. Li, Y.-P. Cao, X.-Q. Feng and H. Gao, Mechanics of morphological instabilities and surface wrinkling in soft materials, A review, *Soft Matter* **8**, 5728–5745 (2012).

22. B.L. Mbanga, F. Ye, J.V. Selinger and R.L.B. Selinger, Modeling elastic instabilities in nematic elastomers. *Physical Review E* **82**, 051701 (4 pages) (2010).

23. J.D. Klayton and J. Knap, A phase field model of deformation twinning: Nonlinear theory and numerical simulations, *Physica D* **240**, 841–858 (2011).

24. J.K. Lee and M.H. Yoo, Elastic strain energy of deformation twinning in tetragonal crystals, *Metallurgical Transactions A* **21A**, 2521–2530 (1990).

25. T.W. Heo, Y. Wang and L.Q. Chen. Spinodal twinning of a deformed crystal, *Philosophical Magazine* **94**, 888–897 (2014).

26. D. Koehn, A. Malthe-Sørenssen and C.W. Passchier, The structure of reactive grain-boundaries under stress containing confined fluids, *Chemical Geology* **230**, 207–219 (2006).

27. P.H. Leo, J.S. and H.J. Jou, A diffuse interface model for microstructural evolution in elastically stressed solids, *Acta Materialia* **46**, 2113–2130 (1998).

28. M.P. Gururajan and T.A. Abinandanan, Phase inversion in two-phase solid systems driven by an elastic modulus mismatch, *Philosophical Magazine* **87**, 5279–5288 (2007).

29. M.J. Borden, C.V. Verhoosel, M.A. Scott, T.J.R. Hughes and C.M. Landis, A phase-field description of dynamic brittle fracture, *Computer Methods in Applied Mechanics and Engineering* **217–220**, 77–95 (2012).

30. W.H. Yang and D.J. Srolovitz, Surface morphology evolution in stressed solids: Surface diffusion controlled crack initiation, *Journal of Mechanics and Physics of Solids* **42**, 1551–1574 (1994).

31. P. Ståhle, C. Bjerkén and A.P. Jivkov, On dissolution driven crack growth, *International Journal of Solids and Structures*, **44**, 1880–1890 (2007).

32. H. Gao, Surface roughening and branching instabilities in dynamic fracture, *Journal of Mechanics and Physics of Solids* **41**, 457–486 (1993).

33. F. Léonard and J. Tersoff, Competing step instabilities at surfaces under stress, *Applied Physics Letters* **83,** 72–74 (2003).

34. L. Angheluta, E. Jettestuen, J. Mathiesen, F. Renard and B. Jamtveit, Stress-driven phase transformation and the roughening of solid-solid interfaces, *Physical Review Letters* **100**, 096105 (4 pages) (2008).

35. J. Colin, Stress-induced destabilization of solidification and melting fronts, *Acta Materialia* **57**, 1454–1458 (2009).

36. D. Walgraef and E.C. Aifantis, Dislocation patterning in fatigued metals as a result of dynamical instabilities, *Journal of Applied Physics* **58**, 688–691 (1985).

37. G. Meng, J. Paulose, D.R. Nelson and V.N. Manoharan, Elastic instability of a crystal growing on a curved surface, *Science* **343**, 634–637 (2014).

38. H. Garcke, R. Nürnberg and V. Styles, Stress- and diffusion-induced interface motion: Modelling and numerical simulations, *European Journal of Applied Mathematics* **18**, 631–657 (2007).

39. A. Artemev, Y. Jin and A.G. Khachaturyan, Three-dimensional phase field model of proper martensitic transfromation, *Acta Materialia* **49**, 1165–1177 (2001).

40. Y.M. Jin, Y.U. Wang and A.G. Khachaturyan, Three-dimensional phase field microelasticity theory and modeling of multiple cracks and voids, *Applied Physics Letters* **79**, 3071–3073 (2001).

41. Y.U. Wang, Y.M. Jin and A.G. Khchaturyan, Phase field microelasticity theory and simulation of multiple voids and cracks in single crystals and polycrystals under applied stress, *Journal of Applied Physics* **91**, 6435–6451 (2002).

42. Y.U. Wang, Y.M. Jin and A.G. Khchaturyan, Phase field microelasticity theory and modeling of elastically and strcuturally inhomogeneous solid, *Journal of Applied Physics* **92**, 1351–1360 (2002).

43. Y.M. Jin, Y.U. Wang and A.G. Khachaturyan, Three-dimensional phase field microelasticity theory of a multivoid multicrack system in an elastically anisotropic body: Model and computer simulations, *Philosophical Magazine* **83**, 1587–1611 (2003).

44. T. Ungár, J. Lendavi and I. Kovács, Determination of the spinodal temperature in a series of Al-Zn (6–21 at.%) alloys, *Philosophical Magazine A* **43**, 927–934 (1981).

45. H. Löffler, C. Eschrich and O. Simmich, Recalculation of several metastable phase lines of the Al-Zn system, *Physica Status Solidi (a)* **113**, 269–275 (1989).

46. Th. H. de Keijser, *On structures developed by spinodal decomposition. The interpretation of the X-ray diffraction and the role of excess vacancies in the coarsening*, PhD thesis, Technical University of Delft, Delft University Press (1977).

47. P.S. Sipling and R.A. Yund, Experimental determination of the coherent solvus for sanidine-high albite, *Americal mineralogist* **61**, 876–906 (1976).

48. T. Dietl, K. Sato, T. Fukushima, A. Bonanni, M. Jamet, A. Barski, S. Kuroda, M. Tanaka, Pham Nam Hai and H. Katayama-Yoshida, Spindoal nanodecomposition in semiconductors doped with transition metals, *Reviews of Modern Physics* **87**, 1311–1377 (2015).

49. A.F. Jankowski, Strain energy effects in the spinodal decomposition of Cu0Ni(Fe) nanolaminate coatings, *Coatings* **5**, 246–262 (2015).

50. C.M. Jantzen, On spinodal decomposition in Fe-free pyroxenes, *American Mineralogist* **69**, 277–282 (1984).

51. A. Lahiri, T.A. Abinandanan, M.P. Gururajan and S. Bhattacharyya, Effect of epitaxial strain on phase separation in thin films, *Philosophical Magazine Letters* **94**, 702–707 (2014).

52. R.D. Twesten, D.M. Follstaedt, S.R. Lee, E.D. Jones, J.L. Reno, J.M. Millunchick, A.G. Norman, S.P. Ahrenkiel and A. Mascarenhas, Characterizing composition modulations in InAs/AlAs short period superlattices, *Physical Review B* **60**, 13619–13635 (1999).

53. N. Liu, J. Tersoff, O. Baklenov, A.L. Holmes Jr., and C.K. Shih, Nonuniform composition profile in In0:5Ga0:5 As alloy quantum dots, *Physical Review Letters* **84**, 334–337 (2000).

54. K. Brunner, Si/Ge nanostructures, *Reports on Progress in Physics* **65**, 27–72 (2002).

55. M.S. Skolnick and D.J. Mowbray, Self-assembled semiconductor quantum dots: Fundamental physics and device applications, *Annual Review of Materials Research* **34**, 181–218 (2004).

56. P. Bhattacharya, S. Ghosh and A.D. Stiff-Roberts, Quantum dot optelectronic devices, *Annual Review of Materials Research* **34**, 1–40 (2004).

57. R. Ragan and H.A. Atwater, Diamond cubic Sn-rich nanocrystals, Synthesis, microstructure and optical properties, *Applied Physics A: Materials Science and Processing* **80**, 1335–1338 (2005).

58. R. Ragan, J.E. Guyer, E. Meserole, M.S. Goorsky and H.A. Atwater, Kinetics governing phase separation of nanostructured Sn_xGe_{1-x} alloys. *Physical Review B* **73**, 235303 (11 pages) (2006).

59. J.R.R. Bortoleto, H.R. Gutiérrez, M.A. Cotta and J. Bettini, Compositional modulation and surface stability in InGaP films: Understanding and controlling surface properties, *Journal of Applied Physics* **101**, 064907 (7 pages) (2007).

60. S. Adhikary and S. Chakrabarti, A detailed investigation on the impact of post-growth annealing on the materials and device characteristics of 35-layer $In_{0.5}Ga_{0.5}As$/GaAs quantum dot infrared photo detector with quaternary $In_{0.21}A_{10.21}Ga_{0.28}As$ capping, *Materials Research Bulletin* **47**, 3317–3322 (2012).

61. J.-N. Aqua, I. Berbezier, L. Favre, T. Frisch and A. Ronda, Growth and self-organization of SiGe nanostructures, *Physics Reports* **522**, 59–189 (2013).

62. M. Myronov, X.-C. Liu, A. Dobbie and D.R. Leadley, Control of epilayer thickness during epitaxial growth of high Ge content strained Ge/SiGe multilayers by RP-CVD, *Journal of Crystal Growth* **318**, 337–340 (2011).

63. X.-C. Liu, R.J.H. Morris, M. Myronov, A. Dobbie and D.R. Leadley, Silicon-germanium interdiffusion in strained Ge/SiGe multiple quantum well structures, *Journal of Physics D: Applied Physics*, **44**, 079501 (1p) (2011).

64. T. Miyazaki, H. Imamura and T. Kozakai, The formation of "γ' precipitate doublets" in Ni-Al alloys and their energetic stability, *Materials Science and Engineering* **54**, 9–15 (1982).

65. M. Doi, T. Miyazaki and T. Wakatsuki, The effect of elastic interaction energy on the morphology of γ' precipitates in nickel-based alloys, *Materials Science and Engineering* **67**, 247–253 (1984).

66. M. Doi, T. Miyazaki and T. Wakatsuki, The effects of elastic interaction energy on the γ' precipitate morphology of continuously cooled nickel base alloys, *Materials Science and Engineering* **74**, 139–145 (1985).

67. M. Doi and T. Miyazaki. γ' precipitate morphology formed under the influence of elastic interaction energies in nickel-base alloys, *Materials Science and Engineering* **78**, 87–94 (1986).

68. M.J. Kaufman, P.W. Voorhees, W.C. Johnson, and F.S. Biancaniello, An elastically induced morphological instability of a misfitting precipitate, *Metallurgical Transactions A* **20A**, 2171–2175 (1989).

69. W.C. Johnson and P.W. Voorhees, Elastically-induced precipitate shape transitions in coherent solids, *Solid State Phenomena* **23–24**, 87–104 (1992).

70. S.J. Yeom, D.Y. Yoon and M.F. Henry, The morphological changes of γ' precipitates in a Ni-8 Al (wt pct) alloy during their coarsening, *Metallurgical Transactions A* **24A**, 1975–1981 (1993).

71. Y.S. Yoo, D.Y. Yoon and M.F. Henry, The effect of elastic misfit strain on the morphological evolution of γ' precipitates in a model ni-base superalloy, *Metals and Materials* **1**, 47–61 (1995).

72. Y.Y. Qiu, The splitting behaviour of γ' particles in Ni-based alloys, *Journal of Alloys and Compounds* **270**, 145–153 (1998).

73. H.A. Calderon, J.G. Cabanas-Moreno and T. Mori, Direct evidence that an apparent splitting pattern of 0 particles in Ni alloys is a stage of coalescence, *Philosophical Magazine Letters* **80**, 669–674 (2000).

74. H.A. Calderon, G. Kostorz, L. Calzado-Lopez, C. Kisielowski and T. Mori, High-resolution electron-microscopy analysis of splitting patterns in Ni alloys, *Philosophical Magazine Letters* **85,** 51–59 (2005).

75. C. Kisielowski, T. Mori and H.A. Calderon, Statistical analysis of γ' quarter split patterns in γ-γ' alloys revealed by high resolution electron microscopy, *Philosophical Magazine Letters* **87**, 33–40 (2007).

76. Y. Yamabe-Mitarai and H. Harada, Formation of a 'splitting pattern' associated with L12 precipitiates in Ir-Nb alloys, *Philosophical Magazine Letters* **82**, 109–118 (2002).

77. J.K. Tien and S.M. Copley, The effect of uniaxial stress on the periodic morphology of coherent γ' precipitates in nickel-base superalloys, *Metallurgical Transactions* **2**, 215–219 (1971).

78. J.K. Tien and S.M. Copley, The effect of orientation and sense of applied uniaxial stress on the morphology of coherent γ' precipitates in stress annealed nickel-base superalloy crystals, *Metallurgical Transactions* **2**, 543–553 (1971).

79. Y.Y. Qiu, The effect of the lattice strains on the directional coarsening of γ' precipitates in Ni-based alloys, *Journal of Alloys and Compounds* **232**, 254–263 (1996).

80. M. Kamaraj, C. Mayr, M. Kolbe and G. Eggeler, On the influence of stress state on in the single crystal superalloy CMSX-6 under conditions of high temperature and low stress creep, *Scripta Materalia* **38**, 589–594 (1998).

81. N. Matan, D.C. Cox, C.M.F. Rae and R.C. Reed, On the kinetics of rafting in CMSX-4 superalloy single crystals, *Acta Materialia* **47**, 2031–2045 (1999).

82. N. Ratel, B. Demé, P. Bastie and P. Caron, In situ SANS investigation of the kinetics of rafting of γ' precipitates in a fourth-generation singlecrystal nickel-based superalloy, *Scripta Materialia* **59**, 1167–1170 (2008).

83. M.S. Titus, A. Suzuki and T.M. Pollock, Creep and directional coarsening in single crystals of new γ'-γ' cobalt-base alloys, *Scripta Materialia* **66**, 574–577 (2012).

84. J.C. Chang and S.M. Allen, Elastic energy changes accompanying gamma-prime rafting in nickel-base superalloys, *Journal of Materials Research* **6**, 1843–1855 (1991).

85. M. Kamaraj, Rafting in single crystal nickel-base superalloys—An overview. *Sādhanā* **28**, 115–128 (2003).

86. L. Shui, S. Tian, T. Jin and Z. Hu, Influence of pre-compression on microstructure and creep characteristic of a single crystal nickel-base superalloy, *Materials Science and Engineering A* **418**, 229–235 (2006).

87. M. Véron, Y. Breéchet and F. Louchet, Strain induced directional coarsening in Ni based superalloys, *Scripta Materialia* **34**, 1883–1886 (1996).

88. M. Véron and P. Bastie, Strain induced directional coarsening in nickel based superalloys: investigation on kinetics using the Small Angle Neutron Scattering (SANS) technique, *Acta Materialia* **45**, 3277–3282 (1997).

89. O. Paris, M. Fährmann, E. Fährmann, T.M. Pollock and P. Fratzl, Early stages of precipitate rafting in a single crystal Ni-Al-Mo model alloy investigated by small-ganle X-ray scattering and TEM, *Acta Materialia* **45**, 1085–1097 (1997).

90. M. Yamashita and K. Kakehi, Tension/compression asymmetry in yield and creep strengths of N–based superalloy with a high amount of tantalum, *Scripta Materialia* **55**, 139–142 (2006).

91. A. Jacques, F. Diologent, P. Caron and P. Bastie, Mechanical behavior of a superalloy with a rafted microstructure, In situ evaluation of the effective stresses and plastic strain rates of each phase, *Materials Science and Engineering A* **483–484**, 568–571 (2008).

92. S. Pierret, T. Etter, A. Evans and H. Van Swygenhoven, Origin of localized rafting in Ni-based single crystal turbine blades before service and its influence on the mechanical properties, *Acta Materialia* **61**, 1478–1488 (2013).

93. C.Y. Chen and W.M. Stobbs, Interfacial segregation and influence of antiphase boundaries on rafting in $\gamma\gamma'$ alloy, *Metallurgical and Materials Transactions A* **35A**, 733–740 (2004).

94. R.J. Asaro and J.W. Tiller, Interface morphology development during stress corrosion cracking: Part I. Via surface diffusion, *Metallurgical Transactions* **3**, 1789–1796 (1972).

95. M.A. Grinfeld, The stress driven instabilities in crystals: Mathematical models and physical manifestations, Technical Report #819, IMA Preprint series (1991).

96. D.J. Srolovitz, On the stability of surfaces of stressed solids, *Acta Metallurgica* **37**, 621–625 (1989).

97. N. Sridhar, J.M. Rickman and D.J. Srolovitz, Multilayer film stability. *Journal of Applied Physics* **82**, 4852–4859 (1997).

98. S. Balibar, H. Alles, and A.Y. Parshin, The surface of helium cyrstals, *Reviews of Modern Physics* **77**, 317–370 (2005).

99. D.E. Jesson, K.M. Chen, S.J. Pennycook, T. Thundat and R.J. Warmack, Mechanism of strain induced roughening and dislocation multiplication in Si_xGe_{1-x} thin films, *Journal of Electronic Materials* **26**, 1039–1047 (1997).

100. J. Berréhar, C. Caroli, C. Lapersonne-Meyer and M. Schott, Surface patterns on single-crystal films under uniaxial stress: Experimental evidence for Grined instability, *Physical Review B* **46**, 13487–13495 (1992).

101. S.W.J. den Brok and J. Morel, The effect of elastic strain on the microstructure of free surfaces of stressed minerals in contact with an aqueous solution, *Geophysical Research Letters* **28**, 603–606 (2001).

102. D. Koehn, J. Arnold, B. Jamtveit and A. Malthe-Sørenssen, Instabilities in stress corrosion and the transition to brittle fracture, *American Journal of Science* **303**, 956–971 (2003).

103. D. Koehn, D.K. Dysthe and B. Jamtveit, Transient dissolution patterns on stressed crystal surfaces, *Ceochemica et Cosmochimica Acta* **68**, 3317–3325 (2004).

104. P.V. Kuznetsov, V.E. Panin and I.V. Petrakova, Grinfeld instability in the formation of a tweed structure at the Al crystal surface under cyclic tension, *Physical Mesomechanics* pages 70–78 (2010).

105. P.V. Kuznetsov, Yu I. Tyurin, I.P. Chernov and T.I. Sigfusson, Grinfeld instability as a mechanism of the formation of self-similar structures on aluminium single-crystal foils under cyclic tension, *Physics of the Solids State* **54**, 2429–2436 (2012).

106. B. Rahmati, W. Jäger, H. Trinkaus, R. Loo, L. Vescan and H. Lüth, Vertical ordering of layers in ge-si multilayers, *Applied Physics A: Materials Science and Processing* **62**, 575–579 (1996).

107. C. Teichert, Self-organization of nanostructures in semiconductor heteroepitaxy, *Physics Resports* **365**, 335–432 (2002).

108. N.K. Sahoo, S. Thakur and M. Senthilkumar, Optical multilayer post growth instabilities: analyses of Gd_2O_3/SiO_2 system in combination with scanning probe force spectroscopy, *Applied Surface Science* **252**, 1520–1537 (2005).

109. C. Duport, P. Nozières and J. Villain, New instability in molecular beam epitaxy, *Physical Review Letters* **74**, 134–137 (1995).

110. D.K. Dysthe, R.A. Wogelius, C.C. Tang and A.A. Nield, Evolution of mineral-fluid interface studies at pressure with synchrotron X-ray technique, *Chemical Geology* **230**, 232–241 (2006).

111. P. Nozières, Shape and growth of crystals, In C Godrèche, editor, *Solids far from equilibrium*, Cambridge University Press, New York (1992).

112. A. Pimpinelli and J. Villain, *Physics of crystal growth*, Cambridge University Press, New York (1999).

113. L.B. Freund and S. Suresh, *Thin film materials: Stress, defect formation and surfae evolution*, Cambridge University Press, New York (2004).

114. V.A. Shchukin and D. Bimberg, Spontaneous ordering of nanostructures on crystal surfaces, *Reviews of Modern Physics* **71**, 1125–1171 (1999).

115. H. Gao and W.D. Nix, Surface roughening of heteroepitaxial thin films, *Annual Review of Materials Research* **29**, 173–209 (1999).

116. J. Stangl, V. Holý and G. Bauer, Structural properties of self-organized semi-conductor nanostructures, *Reviews of Modern Physics* **76**, 725–783 (2004).

117. S. Balibar, H. Alles and A.Y. Parshin, The surface of helium cyrstals, *Reviews of Modern Physics* **77**, 317–370 (2005).

118. J.W. Gibbs, *The collected works of J Willard Gibbs: in two Volumes, Volume I (Thermodynamics)*, Longmans, Green and Co., New York, USA (1928).

119. P.W. Bridgman, On the effect of general mechanical stress on the temperature of transition of two phases, with a discussion of plasticity, *Physical Review* **7**, 215–223 (1916).

120. R. Shuttleworth, The surface tension of solids, *Proceedings of the Physical Society. Section A* **63**, 444–457 (1950).

121. J.W. Cahn, Coherent fluctuations and nucleation in isotropic solids, *Acta Metallurgica* **10**, 907–913 (1962).

122. F.C. Larché and J.W. Cahn, Overview no. 41 The interactions of composition and stress in crystalline solids, *Acta Metallurgica* **33**, 331–357 (1985).

123. W.C. Johnson and J.W. Cahn, Elastically induced shape bifurcations of inclusions, *Acta Metallurgica* **32**, 1925–1933 (1984).

124. A.N. Norris, The energy of a growing elastic surface, *International Journal of Solids and Structures* **35**, 5237–5252 (1998).

125. J.D. Eshelby, The force on an elastic singularity, *Philosophical Transactions of the Royal Society of London, Series A, Mathematical and Physical Sciences* **244**, 87–112 (1951).

126. J.D. Eshelby, The elastic energy-momentum tensor, *Journal of elasticity* **5**, 321–335 (1975).

127. M.E. Gurtin, The nature of configurational forces, *Archive for Rational Mechanics and Analysis* **131**, 67–100 (1995).

128. B.J. Bartholomeusz, The chemical potential at the surface of a nonhydrostatically stressed, defect-free solid, *Philosohpical Magazine A* **71**, 489–495 (1995).

129. M.E. Gurtin, GeneralizedGinzburg-Landau and Cahn-Hilliard equations based on a microforce balance, *Physica D* **92**, 178–192 (1996).

130. A. Miranville, A model of Cahn-Hilliard equation based on a microforce balance, *Comptes Rendus de l'Académie des Sciences—Series I: Mathematical problems in mechanics* **328**, 1247–1252 (1999).

131. D. Gross, S. Kolling, R. Mueller and I. Schmidt, Configurational forces and their application in solid mechanics, *European Journal of Mechanics A/Solids* **22**, 669–692 (2003).

132. S. Li and A. Gupta, On dual configurational forces, *Journal of Elasticity* **84**, 13–31 (2006).

133. G.A. Maugin, *Configurational forces: Thermomechanis, Physics, Mathematics and Numerics*, Modern Mechanics and Mathematics, C.R.C. Press, Chapman & Hall, New York, first edition (2011).

134. M.E. Gurtin, *Configurational forces as basic concepts of continuum physics*, volume 137 of *Applied Mathematical Sciences*, Springer-Verlag, New York, first edition (2000).

135. J.I.D. Alexander and W.C. Johnson, Thermomechanical equilibrium in solid-fluid systems with curved interfaces, *Journal of Applied Physics* **58**, 816–824 (1985).

136. P.H. Leo and R.F. Sekerka, Overview no. 86: The effect of surface stress on crystal-melt and crystal-crystal equilibrium, *Acta Metallurgica* **37**, 3119–3138 (1989).

137. M.E. Gurtin, The dynamics of solid-solid phase transitions 1: Coherent interfaces, *Archive for Rational Mechanics and Analysis* **123**, 305–335 (1993).

138. M. Grinfeld, Stress corrosion and stress induced surface morphology of epitaxial films, *Scanning Microscopy* **8**, 869–882 (1994).

139. C.H. Wu, The chemical potential for stress-driven surface diffusion, *Journal of Mechanics and Physics of Solids* **44**, 2059–2077 (1996).

140. F. Larche and J.W. Cahn, A linear theory of thermochemical equilibrium of solids under stress, *Acta Metallurgica* **21**, 1051–1063 (1973).

141. J.W. Cahn, Surface stress and the chemical equilibrium of small crystals—I. the case of the isotropic surface, *Acta Metallurgica* **28**, 1333–1338 (1980).

142. W.W. Mullins and R.F. Sekerka, On the thermodynamics of crystalline solids, *The Journal of Chemical Physics* **82**, 5192–5202 (1985).

143. W.C. Johnson and J.W.I.D. Alexander, Interfacial conditions for thermomechanical equilibrium in two-phase crystals, *Journal of Applied Physics* **59**, 2735–2746 (1986).

144. W.C. Johnson and C.S. Chiang, Phase equilibrium and stability of elastically stressed heteroepitaxial thin films, *Journal of Applied Physics* **64**, 1155–1165 (1988).

145. M.E. Gurtin and A. Struthers, Multiphase thermomechanics with interfacial structure 3. Evolving phase boundaries int he presence of bulk deformation, *Archive for Rational Mechanics and Analysis* **112**, 97–160 (1990).

146. I, Shimizu, Nonhydrostatic and nonequilibrium thermodynamics of deformable materials, *Journal of Geophysical Research* **97**, 4587–4597 (1992).

147. E. Fried and M.E. Gurtin, Continuum theory of thermally induced phase transitions based on an order parameter, *Physica D* **68**, 326–343 (1993).

148. M.E. Gurtin and P.W. Voorhees, The continuum mechanics of coherent two-phase elastic solids with mass transport, *Proceedings of Royal Society of London A* **440**, 323–343 (1993).

149. E. Fried and M.E. Gurtin, Dynamic solid-solid transitions with phase characterized by an order parameter, *Physica D* **72**, 287–308 (1994).

150. M.E. Gurtin and P. W Voorhees, The thermodynamics of evolving interfaces far from equilibrium, *Acta Materialia* **44**, 235–247 (1996).

151. E. Fried and M.E. Gurtin, Coherent solid-state phase transitions with atomic diffusion: A thermomechanical treatment, *Journal of Statistical Physics* **95**, 1361–1427 (1999).

152. R.F. Sekerka and J.W. Cahn, Solid-liquid equilibrium for nonhydrostatic stress, *Acta Materialia* **52**, 1663–1668 (2004).

153. V. Yeremeyev, A. Freidin and L. Sharipova, The stability of the equilibrium of two-phsae elastic solids, *Journal of Applied Mathematics and Mechanics* **71**, 61–84 (2007).

154. B. Svendsen, Continuum thermodynamic and rate variational formulation of models for extended continua. In B Markert, editor, *Advances in extended & multifield theories for continua*, volume 59 of *Lecture Notes in Applied and Computational Mechancis*, pages 1–18, Springer-Verlag, Berlin (2011).

155. V.I. Levitas, Thermodynamically consistent phase field approach to phase transformations with interface stresses, *Acta Materialia* **61**, 4305–4319 (2013).

156. V.I. Levitas and J.A. Warren, Thermodynamically consistent phase field theory of phase transformations with anisotropic interface energies and stresses, *Physical Review B* **92**, 144106 (16 pages) (2015).

157. S. Nemat-Nasser and M. Hori, *Micromechanics: overall properties of heterogeneous materials*, Elsevier, Amsterdam, second edition (1999).

158. S. Torquato, *Random heterogeneous materials: Microstructure and macroscopic properties,* volume 16 of *Interdisciplinary Applied Mathematics*, Springer-Verlag, New York (2002).

159. A. Anthoine, Derivation of the in-plane elastic characteristics of masonry though homogenization theory, *International Journal of Solids and Structures* **32**, 137–163 (1995).

160. J.C. Michel, H. Moulinec and P. Suquet, Effective properties of composite materials with periodic microstructure: A computational approach, 66 *Computer methods in applied mechanics and engineering* **172**, 109–143 (1999).

161. M.P. Gururajan, *Elastic inhomogeneity effects in microstructures: A phase field study*, PhD thesis, Indian Institute of Science, Bengaluru, INDIA (2006).

162. P. Yu, S.Y. Yu, L.Q. Chen and Q. Du, An iterative-perturbative scheme for treating inhomogeneous elasticity in phase-field methods, *Journal of Computational Physics* **208**, 34–50 (2005).

163. M. Frigo and S. G Johnson, The design and implementation of FFTW3, *Proceedings of the IEEE* **93**, 216–231 (2005).

164. A.G. Khachturyan, S. Semenovskaya and T. Tsakalakos, Elastic strain energy of inhomogeneous solids, *Physical Review B* **52**, 15909–15919 (1995).

165. Y. Wang and A.G. Khachaturyan, Shape instability during precipitate growth in coherent solids, *Acta Metallurgica et Materialia* **43**, 1837– 1857 (1995).

166. D.Y. Li and L.Q. Chen, Shape evolution and splitting of coherent particles under applied stresses, *Acta Materialia* **47**, 247–257 (1999).

167. S.Y. Hu and L.Q. Chen, A phase field model for evolving microstructures with strong elastic inhomogeneity, *Acta Materialia* **49**, 1879–1890 (2001).

168. M.P. Gururajan and T.A. Abinandanan, Phase field study of precipitate rafting under a uniaxial stress, *Acta Materialia* **55**, 5015–5026 (2007).

169. J.E. Hilliard, Spinodal decomposition, In H I Aaronson, editor, *Phase transformations*, ASM, Metals Park, Ohio (1968).

170. J.W. Cahn, On spinodal decomposition, *Acta Metallurgica* **9**, 795–801 (1961).

171. J.W. Cahn, Phase separation by spinodal decomposition in isotropic systems, *Journal of Chemical Physics* **42**, 93–99 (1965).

172. J.W. Cahn, Spinodal decomposition: The 1967 Institute of Metals lecture, *Transactions of the metallurgical society of AIME* **242**, 166–180 (1968).

173. Yu D. Tiapkin, Structural transformation during aging of metal alloys, *Annual Review of Materials Science* **7**, 209–237 (1977).

174. D.A. Porter and K.E. Easterling, *Phase transformations in metals and alloys*, CRC Press, Boca Raton, second edition (1992).

175. W.C. Johnson and P.W. Voorhees, Elastic interaction and stability of misfitting cuboidal inhomogeneities, *Journal of Applied Physics* **61**, 1610–1619 (1987).

176. A.G. Khachaturyan, S.V. Semenovskaya and J.W. Morris, Theoretical analysis of strain-induced shape changes in cubic precipitates during coarsening, *Acta Metallurgica* **36**, 1563–1572 (1988).

177. M. Doi, Coarsening behaviour of coherent precipitates in elastically constrained systems—with particular emphasis on γ' precipitates in nickel-base alloys, *Materials Transactions JIM* **33**, 637–649 (1992).

178. A. Pineau, Influence of uniaxial stress on the morphology of coherent precipitates during coarsening—elastic energy considerations, *Acta Metallurgica* **24**, 559–564 (1976).

179. M.B. Berkenpas, W.C. Johnson, and D.E. Laughlin, The influence of applied stress on precipitate shape and stability, *Journal of Material Research* **1**, 635–645 (1986).

180. W.C. Johnson, Precipitate shape evolution under applied stress—thermodynamics and kinetics, *Metallurgical Transactions A* **18A,** 233–247 (1987).

181. H. Wang and Z. Li, Analytical solution for shape evolution of a coherent precipitate in triaxially stressed solid, *Journal of Materials Research* **19**, 3068–3075 (2004).

182. F.R.N. Nabarro, C.M. Cress and P. Kotschy, The thermodynamic driving force for rafting in superalloys, *Acta Materialia* **44**, 3189–3198 (1996).

183. N. Ratel, G. Bruno, P. Bastie and T. Mori, Plastic strain-induced rafting of γ' precipitates in Ni superalloys: Elasticity analysis, *Acta Materialia* **54,** 5087–5093 (2006).

184. I. Schmidt and D. Gross, Directional coarsening in Ni-base superalloys: analytical results for an elasticity based model, *Proceedings of Royal Society (London) A* **455**, 3085–3106 (1999).

185. J.D. Eshelby, The determination of the elastic field of an ellipsoidal inclusion and related problems, *Proceedings of the Royal Society A. Mathematical, physical and engineering sciences* **241**, 376–396 (1957).

186. P. Müller and A. Saúl, Elastic effects on surface physics, *Surface Science Reports* **54**, 157–258 (2004).

187. H. Emmerich, Modelling elastic effects in epitaxial growth: Stress induced instabilities of epitaxially grown surfaces, *Continuum Mechanics and Thermodynamics* **15**, 197–215 (2003).

188. P. Politi, G. Grenet, A. Marty, A. Ponchet and J. Villain, Instabilities in crystal growth by atomic or molecular beams, *Physics Reports* **324**, 271–404 (2000).

189. M.A. Grinfeld, Stability of interphase boundaries in solid elastic media, *Journal of Applied Mathematics and Mechanics* **51**, 489–496 (1987).

190. M.A. Grinfeld, The stress driven instabilities in crystals: Mathematical models and physical manifestations, Technical report, University of Minnesota, June (1991).

191. W.K. Heidug, A thermodynamic analysis of the conditions of equilibrium at nonhydrostatically stressed and curved solid-fluid interfaces, *Journal of Geophysical Research* **96**, 21909–21921 (1991).

192. M.A. Grinfeld, The stress driven instability in elastic crystals: Mathematical models and physical manifestations, *Journal of Nonlinear Science* **3**, 35–83 (1993).

193. M.A. Grinfeld, On the stress driven instability of thin solid films, *Mechanics Research Communications* **20**, 223–225 (1993).

194. M. Grinfeld, The influence of mass forces on the critical thickness of prestressed he[4] and solid epitaxial films, *Europhysics Letters* **22**, 723–728 (1993).

195. M.A. Grinfeld, The stress driven "rearrangement" instability in crystalline films, *Journal of Intelligent Material Systems and Structures* **4**, 76–81 (1993).

196. L.B. Freund and F. Jonsdottir, Instability of a biaxially stressed thin film on a substrate due to material diffusion over its free surface, *Journal of Mechanics and Physics of Solids* **41**, 1245–1264 (1993).

197. B.J. Spencer, S.H. Davis and P.W. Voorhees, Morphological instability in epitaxially strained dislocation-free solid films: Nonlinear evolution, *Physical Review B* **47**, 9760–9777 (1993).

198. W.K. Heidug and Y.M. Leroy, Geometrical evolution of stressed and curved solid-fluid boundaries 1. Transformation kinetics, *Journal of geophysical research*, **99**, 505–515 (1994).

199. Y.M. Leory and W.K. Heidug, Geometrical evolution of stressed and curved solid-fluid boundaries 2. Stability of cylindrical pores, *Journal of geophysical research* **99**, 571–530 (1994).

200. H. Gao, Some general properties of stress-driven surface evolution in a heteroepitaxial thin film structure, *Journal of Mechanics and Physics of Solids* **42**, 741–772 (1994).

201. L.B. Freund, Evolution of waviness on the surface of a strained elastic solid due to stress-driven diffusion, *International Journal of Solids and Structures* **32**, 911–923 (1995).

202. N. Sridhar, J.M. Rickman and D.J. Srolovitz, Microstructural stability of stressed lamellar and fiber composites, *Acta Materialia* **45**, 2715–2733 (1997).

203. A.N. Norris, Equilibrium, stability and evolution of elastic plates under the combined effects of stress and surface diffusion, *Quarterly Journal of Mechanics and Applied Mathematics* **52**, 283–309 (1999).

204. A. Danescu, The Asaro-Tiller-Grinfeld instability revisited, *International Journal of Solids and Structures* **38**, 4671–4684 (2001).

205. T.V. Savina, P.W. Voorhees and S.H. Davis, The effect of surface stress and wetting layers on morphological instability in epitaxially strained films, *Journal of Applied Physics* **96**, 3127–3133 (2004).

206. C. Misbah, F. Renard, J.-P. Gratier and K. Kassner, Dynamics of a dissolution front for solids under stress, *Geophysical Research Letters* **31**, L06618 (5 pages) (2004).

207. J. Colin, Morphological instabilities of stressed axisymmetrical structures embedded in a matrix: Volume diffusion approach, *Acta Materialia* **52**, 4985–4995 (2004).

208. J. Colin and J. Grilhé, Nonlinear effects of the stress driven rearrangement instability of solid free surfaces, *Journal of Elasticity* **77**, 177–185 (2004).

209. K.G. Kornev and D.J. Srolovitz, Surface stress-driven instabilities of a free film, *Applied Physics Letters* **85**, 2487–2489 (2004).

210. F. Yang and W. Song, Stress-driven morphological instability of axisymmetrical surface coatings, *International Journal of Solids and Structures* **43**, 6767–6782 (2006).

211. F. Yang, Stress-induced surface instability of an elastic layer, *Mechanics of Materials* **38**, 111–118 (2006).

212. J. Colin, On the surface stability of a spherical void embedded in a stressed matrix, *Transactions of the ASME* **74**, 8–12 (2007).

213. P. Müller, Crystal growth and elasticity, *The European Physics Journal Applied Physics* **43**, 271–276 (2008).

214. F.K. Lehner and J. Bataille, Nonequilibrium thermodynamics of pressure solution, *Pure and Applied Geophysics* **122**, 53–85 (1984/85).

215. M.P. Gururajan, Notes of a linear stability analysis (for atg instabilities in thin film assemblies), http://imechanica.org/node/2703. Accessed: 26 April, 2016.

216. A. Ramasubramaniam and V.B. Shenoy, Growth and ordering of SiGe quantum dots on strain patterned substrates, *Transactions of the ASME* **127**, 434–443 (2005).

217. G. Caginalp and E.A. Socolovsky, Efficient computation of a sharp interface by spreading via phase field methods, *Applied Mathematics Letters* **2**, 117–120 (1989).

218. G. Caginalp and E.A. Socolovsky, Computation of sharp phase boundaries by spreading: The planar and spherically symmetric cases, *Journal of Computational Physics* **95**, 85–100 (1991).

219. R. de Borst, Challenges in computational materials science: Multiple scales, multi-physics and evolving discontinuities, *Computational Materials Science* **43**, 1–15, (2008).

220. A.M. Turing, The chemical basis of morphogenesis, *Philosophical Transactions of the Royal Society B* **237**, 37–72 (1952).

221. P.C. Hohenberg and B.I. Halperin, Theory of dynamic critical phenomena, *Reviews of Modern Physics* **49**, 436–479 (1977).

222. P.M. Chaikin and T.C. Lubensky, *Principles of condensed matter physics*, Cambridge University Press, New York, first edition (1995).

223. J.W. Cahn and J.E. Hilliard, Free energy of a non-uniform system I. Interfacial free energy, *Journal of Chemical Physics* **28**(2), 258–267 (1958).

224. W.C. Carter, J.E. Taylor and J.W. Cahn, Variational methods of microstructure-evolution theories, *JOM* **49**, 30–36 (1997).

225. R.E. García C.M. Bishop and W.C. Carter, Thermodynamically consistent variational principles with applications to electrically and magnetically active systems, *Acta Materialia* **52**, 11–21 (2004).

226. J.Z. Zhu, T. Wang, S.H. Zhou, Z.K. Liu, and L.Q. Chen, Quantitative interface models for simulating microstructure evolution, *Acta Materialia* **52**, 833–840 (2004).

227. J.W. Barrett, H. Garcke and R. Nürnberg, Finite element approximation of a phase field model for surface diffusion of coids in a stressed solid, *Mathematics of Computation* **75**, 7–41 (2005).

228. M.A. Zaeem and S. Dj Mesarovic. Finite element method for conserved phase fields: Stress-mediated diffusional phase transformation, *Journal of Computational Physics* **229**, 9135–9149 (2010).

229. L.Q. Chen and J. Shen, Applications of semi-implicit Fourier-spectral method to phase field equations, *Computer Physics Communications* **108**, 147–158 (1998).

230. H. Garcke and D.J.C. Kwak, On asymptotic limits of Cahn-Hilliard systems with elastic misfit, In A Mielke, editor, *Analysis, Modeling and Simulation of Multiscale Problems*, Springer, Brelin (2006).

231. B.G. Chirranjeevi, T.A. Abinandanan and M.P. Gururajan, A phase field study of morphological instabilities in multilayer thin films, *Acta Materialia* **57**, 1060–1067 (2009).

232. R. Mukherjee, T.A. Abinandanan, and M.P. Gururajan, Phase field study of precipitate growth: effect of misfit strain and interface curvature, *Acta Materialia* **57**, 3947–3954 (2009).

233. F.C. Frank, Radially symmetric phase growth controlled by diffusion, *Proceedings of Royal Society of London Series A* **201,** 586–599 (1950).

234. C. Zener, Theory of growth of spherical precipitates from solid solution, *Journal of Applied Physics* **20**, 950–953 (1949).

235. A. Onuki and H. Nishimori, Anomalously slow domain growth due to a modulus inhomogeneity in phase-separating alloys, *Physical Review B* **43**, 13649–13652 (1991).

236. Y. Wang, L.Q. Chen and A.G. Khachaturyan, Kinetics of strain-induced morphological transformtion in cubic alloys with a miscibility gap, *Acta Metallurgical et Materialia* **41**, 279–296 (1993).

237. C. Sagui, A.M. Somoza and R.C. Desai, Spinodal decomposition in an order-disorder phase transition with elastic fields, *Physical Review E* **50**, 4865–4879 (1994).

238. M.E. Thompson and P.W. Voorhees, Spinodal decomposition in elastically anisotropic inhomogeneous systems in the presence of an applied traction, *Modelling and Simulation in Materials Science and Engineering* **5**, 223–244 (1997).

239. Y. Wang, D. Banerjee, C.C. Su and A.G. Khachaturyan, Field kinetic model and computer simulation of precipitation of l12 ordered intermetallics from f.c.c. solid solution, *Acta Materialia* **46**, 2983–3001 (1998).

240. J. Zhu, L.-Q. Chen and J. Shen, Morphological evolution during phase separation and coarsening with strong inhomogeneous elasticity, *Modelling and Simulation in Materials Science and Engineering* **9**, 499–511 (2001).

241. D.J. Seol, S.Y. Hu, Y.L. Li, J. Shen, K.H. Oh and L.Q. Chen, Computer simulation of of spinodal decomposition in constrained films, *Acta Materialia* **51**, 5173–5185 (2003).

242. G. Boussinot, A. Finel and Y. Le Bouar, Phase-field modeling of bimodal microstructrus in nickel-based superalloys, *Acta Materialia* **57**, 921–931 (2009).

243. X. Zhao, R. Duddu, S.P.A. Bordas and J. Qu, Effects of elastic strain energy and interfacial stress on the equilibrium morphology of misfit particles in heterogeneous solids, *Journal of the Mechanics and Physics of Solids* **61**, 1433–1445 (2013).

244. W. Luo, C. Shen and Y. Wang, Nucleatiopn of ordered particles at dislocations and formation of split patterns, *Acta Materialia* **55**, 2579–2586 (2007).

245. D. Banerjee, R. Banerjee and Y. Wang, Formation of split patterns of γ' precipitates in Ni-Al via particle aggregation, *Scripta Materialia* **41**, 1023–1030 (1999).

246. G. Boussinot, Y. Le Bouar and A. Finel, Phase-field simulations with inhomogeneous elasticity: Comparison with an atomic-scale method and application to superalloys, *Acta Materialia* **58**, 4170–4181 (2010).

247. J.K. Lee, A study on coherency strain and precipitate morphology *via* a discrete atom method, *Metallurgical and Materials Transactions A* **27A**, 1449–1459 (1996).

248. P.H. Leo, J.S. Lowengrub and Q. Nie, On an elastically induced splitting instability, *Acta Materialia* **49**, 2761–2772 (2001).

249. P.-R. Cha, D.-H. Lee and S.-H. Chung, Phase-field study for the splitting mechanism of coherent misfitting precipitates in anisotropic elastic media, *Scripta Materialia* **52**, 1241–1245 (2005).

250. J.-Y. Kim, J.-K. Yoon, Y.-C. Kin, H.-K. Suck, K.-B. Kim and P.-R. Cha, Phase field study for self-assemble of the second phase particles in coherent phase transition, *Solid State Phenomena* **124–126**, 583–586 (2007).

251. J.K. Lee, Splitting of coherent precipitates caused by elastic nonequilibrium, *Theoertical and Applied Fracture Mechanics* **33**, 207–217 (2000).

252. J.K. Lee, Studying stress-induced morphological evolution with the Discrete Atom Method, *Journal of Metals* **49**, 37–40 and 58 (1997).

253. J.K. Lee, Elastic stress and microstructural evolution, *Materials Transactions—Japanese Institute of Metals* **39**, 114–132 (1998).

254. J.H. Choy and J.K. Lee, On the shape evolution of a two-dimensional coherent precipitate with a general misfit strain, *Materials Science and Engineering A* **A285**, 195–206 (2000).

255. P. Noziéres, Sixty years of condensed matter physics: An everlasting adventure, *The Annual Review of Condensed Matter Physics* **3**, 1–7 (2012).

256. T. Ichitsubo, D. Koumoto, M. Hirao, K. Tanaka, M. Osawa, T. Yokokawa and H. Harada, Rafting mechanism for ni-base superalloy under external stress: Elastic or elastic-plastic phenomena? *Acta Materialia* **51**, 4033–4044 (2003).

257. T. Tinga, W.A.M. Brekelmans, and M.G.D. Geers, Directional coarsening in nickel-base superalloys and its effect on the mechanical properties, *Computational Materials Sciecne* **47**, 471–481 (2009).

258. K. Tanaka, T. Ichitsubo, K. Kishida, H. Inui and E. Matsubara, Elastic instability condition of the raft structure during creep deformation in nickel-base superalloys, *Acta Materialia* **56**, 3786–3790 (2008).

259. Y. Tsukada, Y. Murata, T. Koyama and M. Morinaga, Phase-field simulation on the formation and collapse processes of the rafted structure in Ni-based superalloys, *Materials Transactions* **49**, 484–488 (2008).

260. D.Y. Li and L.Q. Chen, Computer simulation of morphological evolution and rafting of γ' particles in Ni-based superalloys under applied stresses, *Scripta Materialia* **37**, 1271–1277 (1997).

261. D.Y. Li and L.Q. Chen, Shape evolution and splitting of coherent particles under applied stresses, *Acta Materialia* **47**, 247–257 (1999).

262. A. Gaubert, Y. Le Bouar and A. Finel, Coupling phase field and viscoplasticity to study rafting in ni-based Review-Fsuperalloys, *Philosophical Magazine* **90**, 375–404 (2010).

263. A. Finel, Y. Le Bouar, A. Gaubert and U. Salman, Computational metallurgy and changes of scale—Phase field methods: Microstructures, mechanical properties and complexity, *Comptes Rendus Physique* **11**, 245–256 (2010).

264. K. Kassner and C. Misbah, A phase-field approach for stress-induced instabilities, *Europhysics Letters* **46**, 217–223 (1999).

265. K. Kassner, C. Misbah, J. Müller, J. Kappey and P. Kohlert, Phase-field modeling of stress-induced instabilities, *Physical Review E* **63**, 036117 (27 pages) (2001).

266. K. Kassner, C. Misbah, J. Müller, J. Kappey and P. Kohlert, Phase-field approach to crystal growth in the presence of strain, *Journal of Crystal Growth* **225**, 289–293 (2001).

267. J. Müller and M. Grant, Model of surface instabilities induced by stress, *Physical Review Letters* **82**, 1736–1739 (1999).

268. S.M. Wise, J.S. Lowengrub, J.S. Kim and W.C. Johnson, Efficient phase-field simulation of quantum dot formation in a strained epitaxial film, *Superlattices and Microstructures* **36**, 293–304 (2004).

269. Y.U. Wang, Y.M. Jin and A.G. Khachaturyan, Phase field microelasticity modeling of surface instability of heteroepitaxial thin films, *Acta Materialia* **52**, 81–92 (2004).

270. S.M. Wise, J.S. Lowengrub, J.S. Kim, K. Thornton, P.W. Voorhees and W.C. Johnson, Quantum dot formation on a strain-patterned epitaxial thin film, *Applied Physics Letters* **87**, 133102 (3 pages) (2005).

271. J. Paret, Long-time dynamics of the three-dimensional biaxial Grinfeld instability, *Physical Review E* **71**, 011105 (5 pages) (2005).

272. D.J. Seol, S.Y. Hu, Z.K. Liu, L.Q. Chen, S.G. Kim and K.H. Oh, Phase-field modeling of stress-induced surface instabilities in heteroepitaxial thin films, *Journal of Applied Physics* **98**, 044910 (5 pages) (2005).

273. Y. Ni, L.H. He and A.K. Soh, Three-dimensional phase field simulation for surface roughening of heteroepitaxial films with elastic anisotropy, *Journal of Crystal Growth* **284**, 281–292 (2005).

274. D.-H. Yeon, P.-R. Cha and M. Grant, Phase field model of stress-induced surface instabilities: surface diffusion, *Acta Materialia* **54**, 1623–1630 (2006).

275. J.J. Eggleston, *Phase-field models for thin film growth and ostwald ripening*, PhD thesis, Northwestern University, Evanston, Illinois (2001).

276. J.J. Eggleston and P.W. Voorhees, Ordered growth of nanocrystals via a morphological instability, *Applied Physics Letters* **80**, 306–208 (2002).

277. A. Rätz, A. Ribalta and A. Voigt, Surface evolution of elastically stressed films under deposition by a diffuse interface model, *Journal of Computational Physics* **214**, 187–208 (2006).

278. J.-Y. Kim, J.-K. Yoon and P.-R. Cha, Phase-field model of a morphological instability caused by elastic non-equilibrium, *Journal of the Korean Physical Society* **49**, 1501–1509 (2006).

279. Y. Pang and R. Huang, Effect of elastic anisotropy on surface pattern evolution of epitaxial thin films, *International Journal of Solids and Structures* **46**, 2822–2833 (2009).

280. T. Takaki, T. Hirouchi and Y. Tomita, Phase-field study of interface energy effect on quantum dot morphology, *Journal of Crystal Growth* **310**, 2248–2253 (2008).

281. M.A. Zaeem and S. Dj Mesarovic, Morphological instabilities in thin films: Evolution maps, *Computational Materials Science* **50**, 1030–1036 (2011).

282. A. Danescu and G. Grenet, Vertical correlations in superlattices using the Grinfeld method, *International Journal of Solids and Structures* **40**, 4895–4910 (2003).

283. Z.-F. Huang and R.C. Desai, Stress-driven instability in growing multilayer films, *Physical Review B* **67**, 075416 (19 pages) (2003).

284. J. Paret, Phase-field model of stressed incoherent solid-solid interfaces, http://arxiv.org/abs/cond-mat/0110378, Accessed: 26 April, 2016.

285. C. Shen, N. Zhou and Y. Wang, Phase field modeling of microstructural evolution in solids: Effect of coupling among different extended defects, *Metallurgical and Materials Transactions A* **39A**, 1630–1637 (2008).

286. J.J. Hoyt and M. Haataja, Continuum model of irradiation-induced spinodal decomposition in the presence of dislocations, *Physical Review B* **83**, 174106 (9 pages) (2011).

287. L. Anand, A Cahn-Hilliard-type theory for specified diffusion coupled with large elastic-plastic deformations, *Journal of Mechanics and Physics of Solids* **60**, 1983–2002 (2012).

288. C.V. Di Leo, E. Rejovitzky and L. Anand, A Cahn-Hilliard-type phase-field theory for species diffusion coupled with large elastic deformations: Application to phase-separating li-ion electrode materials, *Journal of Mechanics and Physics of Solids* **70**, 1–29 (2014).

289. S. Song and F. Liu, Kinetic modeling of solid-state partitioning phase transformation with simultaneous misfit accommodation, *Acta Materialia* **108**, 85–97 (2016).

290. Y. Ni, L.H. He and J. Song, Strain-driven instability of a single island and a hexagonal island array on solid substrates, *Surface Science* **553**, 189–197 (2004).

291. X.-L. Gao and H.M. Ma, Solution of eshelby's inclusion problem with a bounded domain and eshelby's tensor for a spherical inclusion in a finite spherical matrix based on a simplified strain gradient elasticity theory, *Journal of the Mechanics and Physics of Solids* **58**, 779–797 (2010).

292. S. Forest, K. Ammar and B. Appolaire, Micromorphic vs. phase-field approaches for gradient viscoplasticity and phase transformations, In B Markert, editor, *Advances in extended & multifield theories for continua*, volume 59 of *Lecture Notes in Applied and Computational Mechancis*, pages 69–88, Springer-Verlag, Berling (2011).

293. L.-T. Gao, X.-Q. Feng and H. Gao, A phase field method for simulating morphological evolution of vesicles in electric fields, *Journal of Computational Physics* **228**, 4162–4181 (2009).

M.P. Gururajan is an Assistant Professor at the Department of Metallurgical Engineering and Materials Science, Indian Institute of Technology Bombay, Mumbai. His research interestes include phase transformations, phase field modelling, thermodynamics and mechanics of materials, atomistic modelling and microstructural evolution. He received his PhD and M Sc (by research) from Department of Metallurgy (currently, Materials Engineering) at Indian Institute of Science, Bengaluru in 2006 and 1999 respectively; he received his M Sc in Materials Science from Anna Unviersity, Chennai in 1996 and B Sc in Physics from Sacred Heart College (Affiliated to Madras University) in 1994. He worked as a post-doctoral fellow at the Materials Science and Engineering Department of Northwestern University, Evanston, IL for nearly two years and spent nearly an year as Assistant Professor at the Applied Mechanics Department in Indian Institute of Technology Delhi, New Delhi. During his PhD, he spent six months at University of Augsburg as a DST-DAAD scholar. His teaching interests include computational laboratory, modelling, simulation and optimization, phase transformation and mathematical methods.

Arka Lahiri is currently pursuing his PhD at the Department of Materials Engineering, Indian Institute of Science, Bengaluru. He received his BE in Metallurgy and Materials Engineering from Bengal Engineering and Science University, Shibpur (currently, Indian Institute of Engineering Science and Technology, Shibpur) in 2009. He obtained his ME from the Department of Materials Engineering, Indian Institute of Science, Bangalore in 2001. Before joining for his PhD, he spent an year in COMSOL Multiphysics as an applications engineer. His research interests include phase transformations and phase field modelling.